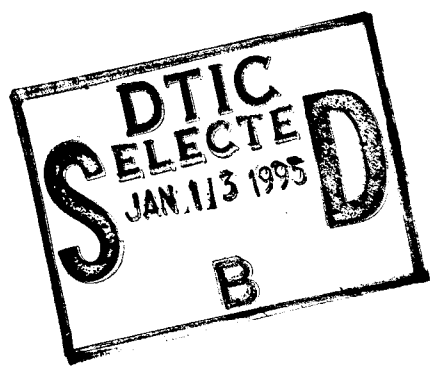




Analysis of Thermal Imagery Collected at Grayling 1 Grayling, Michigan



Salvador Rivera, Jr.

U.S. Army Engineer Waterways Experiment Station
Vicksburg, MS

19950111 116

Original contains color
Copies All DTIC reproductions
will be in black and
white.

DTIC QUANTITY INSPECTED 8

SWOE Report 94-2
January 1994



Analysis of Thermal Imagery Collected at Grayling 1 Grayling, Michigan

Salvador Rivera, Jr.

**U. S. Army Engineer Waterways Experiment Station
Vicksburg, MS**

**SWOE Report 94-2
January 1994**

**Approved for public release;
distribution unlimited**

FOREWORD

SWOE Report 94-2, January 1994, was prepared by S. Rivera, Jr. of U.S. Army Engineer Waterways Experiment Station, Vicksburg, Mississippi.

This report is a contribution to the Smart Weapons Operability Enhancement (SWOE) Program. SWOE is a coordinated, Army, Navy, Marine Corps, Air Force and ARPA program initiated to enhance performance of future smart weapon systems through an integrated process of applying knowledge of the broadest possible range of battlefield conditions.

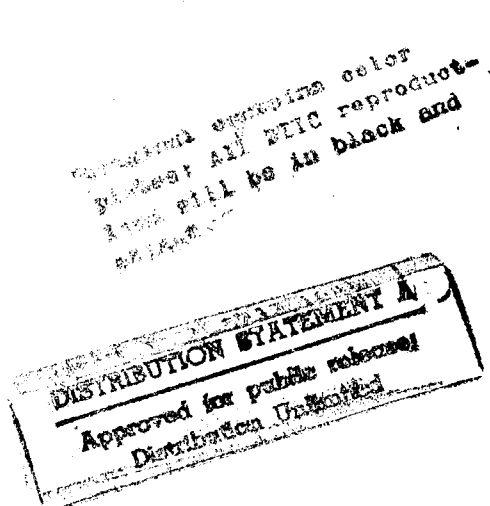
Performance of smart weapons can vary widely, depending on the environment in which the systems operate. Temporal and spatial dynamics significantly impact weapon performance. Testing of developmental weapon systems has been limited to a few selected combinations of targets and environmental conditions, primarily because of the high costs of full-scale field tests and limited access to the areas or events for which performance data are required.

Performance predictions are needed for a broad range of battlefield environmental conditions and targets. Meeting this need takes advantage of significant DoD investments by Army, Navy, Marine Corps and Air Force in 1) basic and applied environmental research, data collection, analysis, modeling and rendering capabilities, 2) extensive target measurement capabilities and geometry models, and 3) currently available computational capabilities. The SWOE program takes advantage of these DoD investments to produce an integrated process, the SWOE Process.

SWOE is developing, validating, and demonstrating the capability of the SWOE Process to handle complex target and environment interactions for a broad range of battlefield conditions. SWOE is providing the DoD smart weapons and autonomous target recognition (ATR) communities with a validated capability to integrate measurements, information bases, modeling, and simulation techniques for complex environments. This is a DoD-wide partnership that works in concert with advanced weapon system developers and major weapon system test and evaluation programs.

The SWOE program started in FY89 under Balanced Technology Initiative (BTI) sponsorship. Present sponsorship is by the U.S. Army Corps of Engineers (lead service), the individual services, and the Joint Test and Evaluation (JT&E) program of the Office of the Director of Test & Evaluation, Office of the Under Secretary of Defense OUSD(A/DT&E).

The Joint Test Director is Dr. J.P. Welsh. The Deputy Test Directors are: (Army) LTC Jerre Wilson and (Air Force) Maj Richard Jennings. The Integration Manager is Mr. Richard Palmer. The Modeling Configuration Manager is Dr. George G. Koenig.



Accession For

NTIS GRA&I	<input checked="" type="checkbox"/>
DTIC TAB	<input type="checkbox"/>
Unannounced	<input type="checkbox"/>

Justification

By _____

Distribution

Availability Codes

Dist	Avail and/or Special
------	-------------------------

A-1

REPORT DOCUMENTATION PAGE			Form Approved OMB No. 0704-0188
<p>Public reporting burden for this collection of information is estimated to average 1 hour per response, including the time for reviewing instructions, searching existing data sources, gathering and maintaining the data needed, and completing and reviewing the collection of information. Send comments regarding this burden estimate or any other aspect of this collection of information, including suggestions for reducing this burden, to Washington Headquarters Services, Directorate for Information Operations and Reports, 1215 Jefferson Davis Highway, Suite 1204, Arlington, VA 22202-4302, and to the Office of Management and Budget, Paperwork Reduction Project (0704-0188), Washington, DC 20503.</p>			
1. AGENCY USE ONLY (Leave blank)	2. REPORT DATE	3. REPORT TYPE AND DATES COVERED	
	January 1994	Final report	
4. TITLE AND SUBTITLE		5. FUNDING NUMBERS	
Analysis of Thermal Imagery Collected at Grayling 1, Grayling, Michigan			
6. AUTHOR(S)			
Salvador Rivera, Jr.			
7. PERFORMING ORGANIZATION NAME(S) AND ADDRESS(ES)		8. PERFORMING ORGANIZATION REPORT NUMBER	
U.S. Army Engineer Waterways Experiment Station Environmental Laboratory 3909 Halls Ferry Road, Vicksburg, MS 39180-6199			
9. SPONSORING/MONITORING AGENCY NAME(S) AND ADDRESS(ES)		10. SPONSORING/MONITORING AGENCY REPORT NUMBER	
U.S. Department of Defense Smart Weapons Operability Enhancement Joint Test and Evaluation Program Office Hanover, NH 03755-1290			
11. SUPPLEMENTARY NOTES			
Available from National Technical Information Service, 5285 Port Royal Road, Springfield, VA 22161.			
12a. DISTRIBUTION / AVAILABILITY STATEMENT		12b. DISTRIBUTION CODE	
Approved for public release; distribution is unlimited.			
13. ABSTRACT (Maximum 200 words)			
<p>The purpose of the Smart Weapons Operability Enhancement (SWOE) Joint Test and Evaluation Program is to validate the SWOE synthetic scene generation procedure. Once validated, this procedure will hopefully change the design-test-redesign approach to smart weapons development, test, and evaluation. Using the SWOE process, smart weapons designers will be able to evaluate their sensor algorithms on simulated scenes with a greater degree of variability than is often presented during the test phase of the design process. The SWOE process will also allow for the smart weapon designs to be evaluated for different environments without the need for expensive and time-consuming data collection exercises.</p> <p>This report is an analysis of thermal data collected by the U.S. Army Engineer Waterways Experiment Station during the Grayling 1 field program 15 September-30 October 1992 to help understand variations in image characteristics using image metrics and to present data in a format that could be used for synthetic image validation tasks.</p> <p>The report also describes in graphical format the meteorological and terrain data at the time the infrared imagery data were collected and correlates measured data with meteorological and terrain data.</p>			
14. SUBJECT TERMS		15. NUMBER OF PAGES	
Grayling, MI		SWOE	
Infrared		75	
Site characterization			
16. PRICE CODE			
17. SECURITY CLASSIFICATION OF REPORT		18. SECURITY CLASSIFICATION OF THIS PAGE	
UNCLASSIFIED		UNCLASSIFIED	
19. SECURITY CLASSIFICATION OF ABSTRACT		20. LIMITATION OF ABSTRACT	

Contents

Preface	iv
1—Introduction.....	1
Background	1
Objectives	2
Scope	2
2—Summary of Image Data Collected.....	3
Image Geometry	3
Description and Summary of Image Data Collected	3
3—Imagery Analysis Procedures.....	5
Image Metrics Computed.....	5
Phase I Image Quality Assurance Analysis.....	5
Phase II Overall Scene Analysis	7
Phase III Scene Component Analysis.....	8
Phase IV Within Pass Scene Analysis	9
4—Correlation of Measured Data With Terrain and Meteorological Data.....	11
Measured Data	11
Meteorological and Terrain Data.....	12
5—Summary of Results.....	16
Bibliography	18
Figures 1-24	20-49
Tables 1-7	50-55
Appendix A Image Data Collection Procedures.....	A1
Appendix B Grayling I Image Metrics.....	B1
Appendix C Instantaneous Meteorological and Terrain Data.....	C1

Preface

The analysis activities reported herein were conducted by the U.S. Army Engineer Waterways Experiment Station (WES) in support of the Smart Weapons Operability Enhancement (SWOE) Joint Test and Evaluation (JT&E) Grayling 1 exercise conducted at Grayling, MI, from 15 September to 25 October 1992. This effort was funded by the Department of Defense SWOE JT&E Program Office, Hanover, NH. Dr. J. Pat Welsh was the Joint Test Director. LTC Jerre W. Wilson was Army Deputy Director, SWOE JT&E.

WES has prepared three related reports in support of the Grayling 1 exercise for the SWOE JT&E Program. These are as follows:

- a. "Grayling 1 Information Base for Generation of Synthetic Thermal Scenes"
- b. "Grayling 1 Site Characterization and Data Summary"
- c. "Analysis of Thermal Imagery Collected at Grayling 1, Grayling, Michigan"

This study was conducted under the general supervision of Dr. John Harrison, Director, Environmental Laboratory (EL), WES, and Mr. H. Roger Hamilton, Acting Chief, Natural Resources Division (NRD), EL, and Mr. Harold W. West, Chief, Environmental Characterization Branch (ECB), NRD, and under the direct supervision of Mr. Charles D. Hahn, WES project coordinator.

Mr. Salvador Rivera, Jr., ECB, prepared this report. Field support was provided by Messrs. Hahn, Thomas Berry, Marvin J. Wooley, David Leese, Clarence Currie, Alfonzo Vasquez, Jerrell R. Ballard, and Stephen Pranger. Mr. Bruce Sabol, ECB, assisted in the image analysis.

At the time of publication of this report, Director of WES was Dr. Robert W. Whalin. Commander was COL Bruce K. Howard, EN.

1 Introduction

The Smart Weapons Operability Enhancement (SWOE) Joint Test and Evaluation (JT&E) Program is a Department of Defense (DOD) coordinated multiservice effort to address problems related to smart weapon system development, test, and evaluation (DT&E) in the worldwide range of battlefield environment conditions. The thrust of the Grayling 1 field exercise was to collect environmental data necessary to generate various synthetic thermal scenes and to collect thermal infrared (IR) image data for use in the validation of the SWOE thermal scene generation procedure.

Background

Future smart weapons systems will be forced to become more "autonomous" because of the ever-shrinking manpower available on the modern battlefield. The typical approach to developing smart weapons has been the test-fix-test methodology for the test and evaluation phases of development. Tests or technology demonstrations are scheduled, and the proposed system is thoroughly tested under various environmental conditions. The results, however, may not be similar if the environmental conditions are changed. Also, the cost of this type of testing is extremely high. The primary thrust of the SWOE JT&E Program is to produce a validated procedure for generation of synthetic thermal and millimeter wave images that accurately model the environmental conditions and can then be processed through the sensor and sensor logic to produce results representative of those from a weapon system captive flight demonstration, all at a much lower cost. An added benefit of this analytical procedure allows the environmental conditions to be changed so that the sensor logic may be evaluated over a variety of background and weather conditions quickly and efficiently.

Objectives

The objectives of this report are as follows:

- a.* To conduct an analysis of thermal data collected by the U.S. Army Engineer Waterways Experiment Station (WES) during the Grayling 1 field program 15 September-30 October 1992 to help understand variations in image characteristics using image metrics, and to present the data in a format that could be used for synthetic image validation tasks.
- b.* To describe in graphical format the meteorological and terrain data at the time the IR imagery data were collected and correlate measured data with meteorological and terrain data.

Scope

The intent of this report is to describe the analysis of WES IR imagery. The data and results are presented in a format useful for synthetic image validation tasks. The final image data are stored in the SWOE program database managed by the SWOE Program Office, Hanover, NH, and made available to the development, test, and evaluation community.

2 Summary of Image Data Collected

Image Geometry

Image data were collected by WES using a ground-based system at Grayling, MI, from September 15 to October 30, 1992. Figure 1 shows a photograph of Site E and surrounding areas that was imaged with a 20-deg lens throughout the field program. Given the importance of features surrounding the Site E area, this study takes into consideration all the information within the field of view (FOV). The dominant terrain features that composed this scene are a large oak tree (deciduous) in the center, three evergreen trees (coniferous) on the left, two small evergreen and one oak tree in the foreground, soil with very short grass, a sandy road or vehicle test track in the background, and a tree line (mixture of coniferous and deciduous trees) just beyond the test track. The approximate image geometry was an azimuth of $76^{\circ}58'55''$ (grid north reference), an elevation angle of $99^{\circ}47'53''$ (measured from vertical), and a slant range of 147.9 m (=distance from WES camera to center of Site E area imaged). The camera was located at universal transverse Mercator (UTM) coordinates 687083E 4951896N and at a height of 17.2 m above the ground surface.

Description and Summary of Image Data Collected

The WES imaging equipment consisted of a far infrared (long wave band (LWB)) and a midinfrared (short wave band (SWB)) thermal imager. All the analysis on the SWB imagery includes the reflected and emitted component. An LWB and SWB IR image of Site E and surrounding area are shown in Figures 2 and 3, respectively. The WES thermal cameras had 20-deg FOV lenses; the specifications for these cameras are shown in

Table 1. Appendix A offers a general explanation of the image data collection procedure; another report provides a more in-depth explanation.¹

The imaging schedule (see Table 2) was arranged so that 107 2-hr image data collection missions would be accomplished during the SWOE Grayling 1 effort. One image frame was collected per second for 10 sec. These imaging periods were conducted at 5-min intervals throughout the established 2-hr data collection period. For program purposes, every 5-min time count was known as a pass (or section); at the end of a 2-hr imaging, there were 25 passes. One particular pass and frame was randomly selected and designated the critical frame. All the analysis in these reports is based on the critical frame.

The 107 data collection missions were executed under a broad variety of meteorological conditions. Another report gives a summary of meteorological data.¹ Of the total missions, 52 percent were accomplished during nighttime conditions. Figure 4 illustrates a frequency histogram of the air temperature values during the critical frames. The figure reflects that 14 percent of the missions were executed under temperatures below freezing, 41 percent at air temperatures between 0 and 10 °C, 42 percent at air temperatures between 10 and 20 °C, and 3 percent at air temperatures above 20 °C. By 04 October, the leaves on the deciduous trees within the site had started to turn color (red); by 13 October, the leaves were completely red. Between the dates 16 October-21 October, there were some critical frames with either snowfall/snow precipitation, snow cover on the ground and snow collected on the trees or no snow at all.

¹ Hahn, C. D., and Berry, T. E. (1994). "Grayling 1 site characterization and data summary," Technical Report prepared by the U.S. Army Engineer Waterways Experiment Station, Vicksburg, MS, for the Smart Weapons Operability Enhancement Joint Test and Evaluation Program Office, Hanover, NH.

3 Imagery Analysis Procedures

Image Metrics Computed

Image metrics were used to quantify the distribution of specific features within a digital image. Nine different scene metrics were computed in this study. All of these characterize the data-space distribution of temperature in degrees Celsius. Processing was initiated by generating histograms of digital level values within the designated region. Eight measures are computed from the histogram: the minimum value (MIN), the 5-percentile value (PERC_05), the median value (MEDIAN), the mode (MODE), the 95-percentile value (PERC_95), the maximum value (MAX), and the difference between the 95- and 5-percentile (RNG_90). The first and second moments of the distribution of digital level values within the designated region (mean and standard deviation) are also computed. Results were converted to temperature by substituting them (and camera calibration constant) into Planck's equation.

Phase I: Image Quality Assurance Analysis

A procedure was employed to verify the accuracy of the radiometric temperature estimates and to ensure that the manual settings of all images were within dynamic range. This procedure also allowed identification and elimination of image data with noise other than that resulting from the scanner. This image noise was possible given the numerous external electric sources operating at the same time at the site where data were collected. Figure 5 shows a flowchart describing the several image quality tests used to ensure that the final imagery set was within calibration, within dynamic range, and without noise. Imagery that did not pass these tests was discarded. At the end, a confirmation analysis was performed by processing WES and Atmospheric Research Laboratory (ARL) IR data (both wave bands) and comparing the mean temperature and standard deviation of the features for all the critical frames. Assuming that both systems are operating at factory calibration, the mean temperature difference of the features

should be within ± 3 °C and the standard deviation difference within ± 0.5 °C.

At the beginning and end of each of the 107 missions (refer to Appendix A for more details), an IR image of the four active blackbodies was taken, along with the actual (truth) temperature of each blackbody. The purpose was to implement the first image quality test, which consists of verifying that the absolute error between the actual temperature and estimated radiometric temperature is within ± 3 °C, which was the criteria for acceptance. A linear regression analysis was applied to the data that did not meet the criteria for acceptance. Data were accepted if they met the criteria for acceptance after the linear regression. Otherwise, the data were discarded. This analysis was applied to blackbody data collected before 12OCT92:14:00 because the remaining data was considered spurious. The next paragraphs will show that IR data (both wave bands) collected after 12OCT92:14:00 met calibration criteria.

Figure 6a shows a plot of the absolute error versus date for all the active blackbody data in the LWB collected throughout the field exercise. Each of the plots shows a band (horizontal lines) of ± 3 °C, the calibration criteria for acceptance. This plot indicates that most of the data met the criteria for acceptance. Figure 6b shows a frequency histogram of the absolute error, indicating that 99 percent of the data met the criteria for acceptance. Therefore, the factory calibration of the LWB camera needed no correction.

Figure 7a shows a plot of the absolute error versus date for all the blackbody data in the SWB collected during the field exercise. This plot indicates that most of the data is within ± 3 °C, with the exception of the imagery collected before 29SEP92:02:00. Figure 7b is a frequency histogram of the absolute error, showing that 93 percent of the data are within the criteria for acceptance. A linear regression was performed on the data collected before 29SEP92:02:00 to obtain an equation to correct the data. Figure 8 offers the result of this analysis (Figure 8a) where 98 percent of the data (Figure 8b) subsequently satisfied the criteria for acceptance. Imagery collected before 29SEP92:02:00 was corrected using this equation: (NEW_TEMP=0.984*OLD_TEMP-2.269).

As part of the second image quality test, all the imagery collected were checked, given that cameras require manual setting of the levels and ranges, to ensure that the imagery were within dynamic range. Images with more than 2 percent of the brightness values (8 bit radiometric resolution) less than 5 or greater than 250 were rejected.

The third and last image quality test consisted of visually identifying image data with noise other than the noise due to the scanner. Once identified, these image data were processed using a Fast Fourier Transform (FFT) transforming them to the frequency domain. Low pass filter was then applied to eliminate all undesired high frequencies (noise). The

image data were then transformed back to the spatial domain. If the noise test failed, the image data were rejected.

At the end, a confirmation analysis was performed by processing WES and ARL IR data (both wave bands) and comparing the feature's mean temperature and standard deviation for all the critical frames. Assuming that both systems are operating at factory calibration, the feature's mean temperature difference should be within ± 3 °C and the feature's standard deviation difference within ± 0.5 °C. Figures 9-12 show for the features grassy area, coniferous tree, deciduous tree, and test track, respectively, histograms of the difference in mean temperature and standard deviation between WES and ARL IR data. Figures 9a-12a show a histogram for the LWB data of frequency versus feature mean temperature difference. Figures 9b-12b show a histogram for the LWB data of frequency versus feature standard deviation difference. Figures 9c-12c show a histogram for the SWB data of frequency versus feature mean temperature difference. Figures 9d-12d show a histogram for the SWB data of frequency versus feature standard deviation difference. These histograms reflect that, for any feature/wave band combination, the mean temperature difference is within ± 3 °C (WES and ARL absolute temperature accuracy is ± 3 °C and ± 1 °C, respectively). The standard deviation difference is within ± 0.5 °C. After confirmation results were examined, the LWB and SWB IR data were used for further analysis.

Table 3 summarizes data based on 107 test missions. In the LWB, 83 percent of the data was considered acceptable; in the SWB, 79 percent of the data was considered acceptable.

Phase II: Overall Scene Analysis

Appendix B shows a listing of the image metric database for the critical frames. The information contained in the listing includes the date-time when the critical image was collected (IMAGE_DT), date-time when the mission was started (MISSN_DT), wave band to which the image belongs (WAVEBAND), mission number (MISSION), pass number (PASS), frame number (FRAME), and nine image metrics.

One of the first steps when analyzing IR image data is to determine the mean temperature and variability. Figure 13 shows a three-dimensional (3-D) plot of the frequency count of the image mean temperature and standard deviation (degrees Celsius) for all the critical frame data. For the LWB data (Figure 13a), 83 percent of the image data had a mean temperature between 0.0 and 20.0 °C. Also, 80 percent of the image data show very little thermal variation with standard deviation between 0.0 and 1.0 °C. The two highest peaks had a mean and standard deviation of the following (respectively):

- (1) 0 and 1 °C (8 percent of data).
- (2) 7.5 and 1 °C (10 percent of data).

In the SWB data (Figure 13b) 90 percent of the image data had a mean temperature between 5.0 and 20.0 °C. Also, 86 percent of the image data showed very little thermal variation, with standard deviation between 0.0 and 1.0 °C. The six highest peaks had a mean and standard deviation of the following (respectively):

- (1) 5 and 0 °C (9 percent of data).
- (2) 12.5 and 0 °C (10 percent of data).
- (3) 20 and 0 °C (9 percent of data).
- (4) 10 and 1 °C (9 percent of data).
- (5) 12.5 and 1 °C (9 percent of data).
- (6) 15 and 1 °C (9 percent of data).

To illustrate variability, Figure 14 shows a frequency count histogram of the temperature range (RNG_90) of all the data processed for both wave bands. In the LWB, 90 percent of the data had a temperature range of 6 °C or less, while 90 percent of the SWB data showed a temperature range of 5 °C or less.

Phase III: Scene Component Analysis

This analysis consisted of selecting several features/areas of interest (FOI or AOI) that were considered homogeneous within the scene (see Figure 1). Mean temperature and standard deviation were first computed for the AOI; analysis included a large red oak tree (deciduous) near the center of the scene, the smaller groups of evergreen trees (coniferous) to the left of the oak tree, a grassy area in the foreground, and a stretch of the test track in the background of the scene. These statistics were computed using all the pixels within the polygons enclosing each of the features. A database was generated with the mean temperature and the standard deviation of the features (grassy area, coniferous tree, deciduous tree, and test track) in Site E and surrounding areas.

For each wave band, the air temperature and the feature's mean temperatures bounded by one standard deviation were plotted (Figures 15a and 15b, respectively). In both wave bands, the grassy area followed by the test track exhibited warmer temperatures and more thermal variability than the deciduous and coniferous trees. The deciduous and coniferous trees exhibited very similar temperatures throughout the data collection time. After 07 October, all the features exhibited minimal thermal variability; during the same time, the air temperature remained cool (average 5 °C) until 23 October. In general, comparing the plots for each wave band indicates that the SWB data exhibited warmer temperatures and more thermal

variability than the LWB data. Comparing the air temperature with the feature's mean temperature indicates that the temperature of the coniferous and deciduous trees tracked the air temperature very closely, although it was more noticeable in the LWB than in the SWB. Appendix B shows a listing of the image metrics computed on the entire image and the five features composing the image.

Phase IV: Within Pass Scene Analysis

The purpose of this analysis was to determine whether the scene changed significantly during the 10-sec imaging period. This analysis consisted of performing pairwise comparison of the cumulative percent distribution of all possible images within the 10-sec period. The Kolmogorov-Smirnov¹ like test was used to detect differences. Results were plotted as average Smirnov test statistics as a function of a time lag between images, and the trend of the line was used to determine whether these 10 images change significantly with time. The following procedure was used for 10 images collected 10 sec apart:

- a. A frequency histogram of the digital value distribution of each of the 10 images was first generated.
- b. The distributions were then normalized by constructing a cumulative percent histogram from the frequency histogram of the 10 images.
- c. Using the cumulative percent histogram, the greatest vertical distance (T) was computed for every possible combination. Figure 16 is an illustration of a frequency histogram and cumulative percent histogram for two images. Table 4 was produced by computing T for every possible combination among all 10 images.
- d. The adjacent observations were obtained for the nine possible lag times.
- e. All observations were averaged for a particular lag time, and a plot was generated of the average T versus lag time.
- f. The trend (of the line) was analyzed to determine whether the line changed significantly in 10 sec and whether or not it was dependent on time.

Lag time (seconds)	Number of observations
1	9
2	8
3	7
4	6
5	5
6	4
7	3
8	2
9	1
Total number of observations	45

¹ Conover, W. J. (1971). *Practical nonparametrics statistics*. John Wiley and Sons, Inc., New York.

As part of the analysis, the missions were also grouped by the type of weather conditions in which they occurred. The four weather condition groups were sunny day, partly cloudy day, cloudy day, and nighttime. For each group, three image missions were selected; critical passes (10 images each) were analyzed for each of those selected.

Figures 17 and 18 show, for the LWB and SWB, respectively, a plot for each of the four weather condition groups. Each plot shows the trend of T with respect to time for each critical pass. In the SWB (Figure 18), the trend illustrates that the critical pass images from mission No. 71 (a partly cloudy day) changed significantly with time. All the other critical pass images at different weather conditions showed no change with time. The same observations were noticed in the LWB (Figure 17).

4 Correlation of Measured Data with Terrain and Meteorological Data

IR data were collected under a broad variety of meteorological conditions that affects the IR signatures of the imaged features within Site E and surrounding areas (Figure 1). Some meteorological factors that occurred during the data collection were dense fog, rain and snow precipitation. These factors affect (block) the feature's infrared energy being measured by the scanner. High content of soil moisture because of rain and snow precipitation as well as snow accumulation on trees, grass, and ground also affects IR signatures on natural background materials. During the data collection period, there was a wide variety of sunny, partly cloudy, and cloudy days. Air temperature, relative humidity, wind speed, and wind direction also exhibited a wide range of values. The purpose of this section is to illustrate by graphics and tables the meteorological and terrain conditions that occurred during the collection of the IR imagery. In addition, this section will correlate the mean temperature and standard deviation of the critical frame imagery with the meteorological and terrain conditions.

Measured Data

Figure 19 illustrates, for most of the 107 critical frames, the image mean apparent temperature bounded by the standard deviation in the LWB and SWB. The image mean apparent temperature for both wave bands exhibited a wide range of temperatures fluctuating approximately between -7 and 27 °C. Cool temperatures are grouped between missions No. 70 (12 October 1992) and No. 100 (22 October 1992), while warm temperatures are grouped between missions No. 15 (19 September 1992) and No. 55 (06 October 1992). The imagery in both wave bands exhibited a maximum thermal variability between missions No. 10 (17 September 1992) and No. 55 (06 October 1992).

A scene component analysis was performed in which each of the features was examined individually (See Scene Component Analysis section for more information). Figure 15 shows the mean temperature of the features bounded by standard deviation for the four features composing the image (grassy area, coniferous tree, deciduous tree, and test track). The mean temperature for all the features fluctuates considerably throughout the 45 days of data collection (-8 to 30 °C). The features exhibit more thermal variability in the SWB data than in the LWB data.

Meteorological and Terrain Data

During the test, the WES team recorded most of the daytime missions on VHS videotapes. These videotapes were used to make color hardcopy pictures of Site E and surrounding areas at the moment the critical frame was collected (WES visual). Figure 20 illustrates physical changes that occurred at Site E and surrounding areas throughout the test period. The date and time are included on each visual photo.

Some of the most important events that occurred were as follows:

- a. 20SEP,15:28 - Leaves on deciduous trees and others are green.
- b. 21SEP,11:57 - A dense foggy day.
- c. 05OCT,15:43 - Leaves on deciduous trees beginning to turn red.
- d. 12OCT,10:48 - Most of the deciduous tree leaves are red
- e. 18OCT,08:43 - Snow covers the ground, accumulated on trees.
- f. 19OCT,08:58 - Snow precipitation.
- g. 19OCT,17:58 - Snow melted on the bare ground patches.
- h. 20OCT,12:00 - Snow precipitation.
- i. 21OCT,11:34 - Snow accumulated on the ground, trees, and grass.
- j. 22OCT,16:19 - Normal sunny day conditions.

Figure 21 shows the WES-measured meteorological conditions throughout the test period. The total solar radiation (0.4- to 0.7- μ m range; another report provides instrument specifications¹) measured was used to

¹ Hahn, C. D., and Berry, T. E. (1994). "Grayling 1 site characterization and data summary," Technical Report prepared by the U.S. Army Engineer Waterways Experiment Station, Vicksburg, MS, for the Smart Weapons Operability Enhancement Joint Test and Evaluation Program Office, Hanover, NH.

illustrate cloud cover. Solar radiation is the real driving factor during the day, especially for the SWB sensor if the hemispherical albedo is relatively high. The test started and ended with some partly cloudy days (Figure 21a). During the test, there were many sunny days as well as partly cloudy and cloudy days. The dates 25-27 September are good samples of sunny days; the dates 15-17 September were partly cloudy days. The dates 21 September, 15 October, and 20 October were very cloudy days. From the beginning of the test, the air temperature (Figure 21a) exhibited peaks (at noon) and valleys (early morning and late evening) until 08 October. Those days exhibited some of the warmer air temperatures. Between 09 October and 22 October, the air temperature decreased and increased with a small slope and eventually dropped below freezing. At the end of the test (23 October), the air temperature was quite high.

The barometric pressure (Figure 21b) showed very little fluctuation (970 to 1,010 mb) during the duration of the test. On sunny days, the relative humidity (Figure 21b) dropped to 40 percent, while on cloudy days dropped to 90 percent. The wind speed (Figure 21c) fluctuated between 0.2 and 3.5 m/sec. The dates with the higher wind speed occurred between 16 September and 09 October. Meanwhile, the dates with the slower wind speed occurred on the dates 15 September, 29 September, 30 September, and 15 October. The wind direction (Figure 21c) most of the time blew from the west (0°=NORTH and 90°=EAST).

Visibility (Figure 21d) varied appreciably within a 24-hr period. For example, during the first 8 hr of 15 September, the visibility was a very low 0.2 km; then it quickly changed to 22 km. There were a few days with rain as well as snow precipitation (Figure 21d). Most of the rain occurred on 17 September (35 mm/hr), meanwhile the dates 16 October, 18 October, and 20 October exhibited a considerable amount of snow precipitation.

Figure 22 shows the instantaneous meteorological conditions at the moment the critical frames were collected. The air temperature (Figure 22a) fluctuated between -5 and 25 °C with a mean temperature of 9.14 °C and a variability of 7.12 °C. Also, 52 percent of the missions were executed at night or during low levels of solar radiation (Figure 22a). Relative humidity (Figure 22b) fluctuated between 100 and 44 percent. Of the critical frames, 44 percent exhibited relative humidity of 100 percent, and 74 percent exhibited relative humidity greater than 80 percent. The barometric pressure (Figure 22b) exhibited a small range of values fluctuating between 980 and 1,005 mb. The average wind speed (Figure 22c) was 1.5 m/sec with wind speed varying between 0 and 3 m/sec. The direction in which the wind was blowing (Figure 22c) for each critical frame showed a spread between 0 and 360° (0°=NORTH and 9°=EAST). Very few missions exhibited either snow or rain precipitation (Figure 22d). Rain precipitation occurred during mission No. 8 (12mm/hr), while mission No. 92 had considerable snow precipitation (6.2 mm/hr). Appendix C shows a listing of all the missions and the instantaneous meteorological conditions, accumulated (last 12 hr) rain and snow precipitation, average (for the last 12 hr)

solar radiation and air temperature, and image mean temperature and standard deviation.

Visibility data, precipitation data, and WES visual (video) data were used to detect dense fog, snow, or rain precipitation during the critical frames. Although the terrain area imaged was only a short distance (150 m), visibility with less than 5 km has some effect on the measured IR signatures. Table 5 lists all the missions where the visibility was less than 5 km. The information in this table contains mission number, collection time, visibility distance, visual (video) data availability, and type of atmospheric condition along the transmittance path.

Precipitation data and soil moisture data were used to determine the possibility of the ground being wet during the critical frame collection. The average solar radiation, air temperature, and accumulated precipitation were computed (Figure 23) for the last 12 hr prior to the critical frames. There is a high possibility that the ground remained wet during some of the missions between No. 61 and No. 95 because of precipitation accumulation and low averages of both solar radiation and air temperature (during the last 12 hr). Table 6 shows the missions with accumulated precipitation greater than 5 mm/hr during the previous 12 hr and provides data on the average solar radiation and air temperature during the previous 12 hr and the Troxler and Speedy soil moisture data for Sites E1/E2.

The Site E area was divided (in two parts) where the left side was referred to as Site E1 and the right side as Site E2. Soil moisture data were collected at each site using the Troxler Model 4640 Thin Layer Density Gauge and the Soiltest Speedy Moisture Gauge. The Troxler device determines soil moisture by measuring the backscattering of low-level radiation from the surface of the soil. The Soiltest Speedy Moisture Gauge determines the moisture by combining a measured amount of soil with a measured amount of calcium carbide. The moisture in the soil reacts with the calcium carbide to produce acetylene gas. A pressure gauge on the Speedy then reads the gas pressure, and the reading is converted to a percent moisture. An important distinction between these two instruments is that the Troxler measures the moisture in a thin soil layer at or near the surface, while the Speedy determines the moisture based on a specific depth volume of soil. Speedy soil samples were collected from the area measured with the Troxler device within a 0- to 2.5-cm depth layer. Figure 24 illustrates the soil moisture data collected at Sites E1/E2 with both instruments. See "Grayling 1 Site Characterization and Data Summary" for more information about soil composition, soil moisture data, and instrumentation.¹

¹ Hahn, C. D., and Berry, T. E. (1994). "Grayling 1 site characterization and data summary," Technical Report prepared by the U.S. Army Engineer Waterways Experiment Station, Vicksburg, MS, for the Smart Weapons Operability Enhancement Joint Test and Evaluation Program Office, Hanover, NH.

Snow precipitation data and WES visual data were used to determine the possibility of snow precipitation along the path during the critical frame collection. It could not be accurately determined whether there was snow precipitation for those critical frames without WES visual data. For these cases, the amount of snow precipitation, within the hour when the critical frame was collected, was used as an indicator. The following missions exhibited snow precipitation.

Mission Number	Collection Date-Time	Precipitation Rate, mm/hr	Source of Information
82	16OCT92:17:00:06	1.98	Visual observation and snow precipitation gauge
83	17OCT92:07:10:10	0.28	Snow precipitation gauge
88	19OCT92:03:25:09	0.04	Snow precipitation gauge
89	19OCT92:09:00:08	0.03	Visual observation and snow precipitation gauge
92	20OCT92:12:00:02	6.71	Visual observation and snow precipitation gauge

Snow precipitation data and WES visual data were used to determine whether there was snow covering the terrain features (trees, grass, and bare ground) at the critical frame collection. Table 7 lists the missions and features containing snow. The amount of snow accumulated by each feature could not be determined.

5 Summary of Results

The WES LWB IR camera needed no calibration correction because the camera was operating within factory specification (± 3 °C). A linear regression was performed to obtain an equation that would correct the WES SWB infrared data so that the blackbody temperature error would be within ± 3 °C. Using that equation corrected the SWB IR data from 93 to 98 percent within ± 3 °C. WES IR imagery collected at Grayling 1 exercise showed that 83 and 79 percent, respectively, of the LWB and SWB data were considered valid.

An analysis was performed by processing WES and ARL IR data (both wave bands) and comparing the mean temperature and standard deviation of the features for all the critical frames. The results showed that for any feature/wave band combination, the mean temperature difference is within ± 3 °C (WES and ARL absolute temperature accuracy is ± 3 and ± 1 °C, respectively). The standard deviation difference is within ± 0.5 °C.

Several global image metrics were computed and stored in a database for the Grayling 1 imagery. These image metrics include minimum, maximum, mean, median, mode, 5-percentile, 95-percentile, range-90, and standard deviation. In both wave bands, the terrain scene measured indicated very little thermal variability.

In the LWB, 83 percent of the WES imagery showed a mean temperature between 0 and 20 °C. Also, 80 percent of the imagery had a standard deviation between 0.0 and 1.0 °C. In addition, 90 percent of the data showed a temperature range of 6 °C or less.

In the SWB, 90 percent of the imagery showed a mean temperature between 5 and 20 °C. Also, 86 percent of the imagery had a standard deviation between 0.0 and 1.0 °C. Moreover, 90 percent of the data indicated a temperature range of 5 °C or less.

A database was generated with the mean temperature and standard deviation of several natural background features (grassy area, coniferous tree, deciduous tree, and road or test track) within Site E and surrounding areas. This database is considered useful for understanding the variations in IR image signatures to be used in SWOE synthetic image validation

tasks. In both wave bands, the grassy area followed by the test track exhibited warmer temperatures and more thermal variability than the coniferous and deciduous trees. Also, the coniferous and deciduous trees exhibited very similar temperatures. The SWB data exhibited warmer temperatures and more thermal variability than the LWB data.

With the exception of 1 case in 11, a Kolmogorov-Smirnov like test showed no time-dependent changes in the imagery collected within 10-sec sampling periods for both wave bands.

IR data were collected under a broad variety of meteorological conditions that affected the IR signatures of the imaged terrain features (grassy area, trees, test track, etc.) within Site E and surrounding areas. Some of the meteorological factors that occurred during the data collection missions were dense fog, rain, and snow precipitation. High soil moisture content because of rain and snow precipitation as well as snow accumulation also affected measured IR signatures of terrain features. During the data collection period, there was a wide variety of sunny, partly cloudy, and cloudy days. Air temperature, relative humidity, wind speed, and wind direction also exhibited a wide range of values. Based on 107 missions, 14 percent of the missions were executed under temperatures below freezing, 41 percent at air temperatures between 0 and 10 °C, 42 percent at air temperatures between 10 and 20 °C, and 3 percent at air temperatures above 20 °C. Also, 52 percent of the missions were accomplished during nighttime conditions. Each of these parameters are associated with the critical frame.

WES equipment (infrared scanners, meteorological station, global positioning system, soil moisture equipment, and others) proved to be reliable and effective for site characterization and measurements.

Bibliography

Balick, L. K. (1992). "Deciduous forest scene complexity in high resolution multispectral scanner imagery," Technical Report EL-92-26, U.S. Army Engineer Waterways Experiment Station, Vicksburg, MS.

Ballard, J. (1994). "Grayling 1 information base for generation of synthetic thermal scenes," Technical Report prepared by the U.S. Army Engineer Waterways Experiment Station, Vicksburg, MS, for the Smart Weapons Operability Enhancement Joint Test and Evaluation Program Office, Hanover, NH.

Beard, J., Clark, L., and Velton, V. (1985). "Characterization of ATR performance in relation to image measurements," Unpublished paper, AFWAL/AARF, Wright Patterson AFB, OH.

Berry, T., Rivera, S., Jr., and Sabol, B. (1993). "Environmental characterization for target acquisition; Report 1, Site description and measurements," Technical Report EL-93-9, U.S. Army Engineer Waterways Experiment Station, Vicksburg, MS.

Carlson, G. E., and Radford, D. J. (1986). "Image metrics study," University of Missouri, Electrical Engineering Department Report No. CSR 86-2, Rolla, MO.

Conover, W. J. (1971). *Practical nonparametrics statistics*. John Wiley and Sons, Inc., New York.

Hahn, C. D., and Berry, T. E. (1994). "Grayling 1 site characterization and data summary," Technical Report prepared by the U.S. Army Engineer Waterways Experiment Station, Vicksburg, MS, for the Smart Weapons Operability Enhancement Joint Test and Evaluation Program Office, Hanover, NH.

Sabol, B. M., and Hall, K. G. (1990). "Image metrics approach to understanding effects of terrain and environment on performance of thermal target acquisition systems," SPIE 1312, 310-329.

Sabol, B., and Rivera, S., Jr. (1991). "Analysis of scene conditions at the light helicopter target acquisition subsystem demonstration/validation, Yuma Proving Ground, Arizona, September 1990," Technical Report EL-91-5, U.S. Army Engineer Waterways Experiment Station, Vicksburg, MS.

SAS Institute, Inc. (1988). *SAS procedures guide*, Release 6.03 ed., SAS Institute, Inc., Cary, NC.

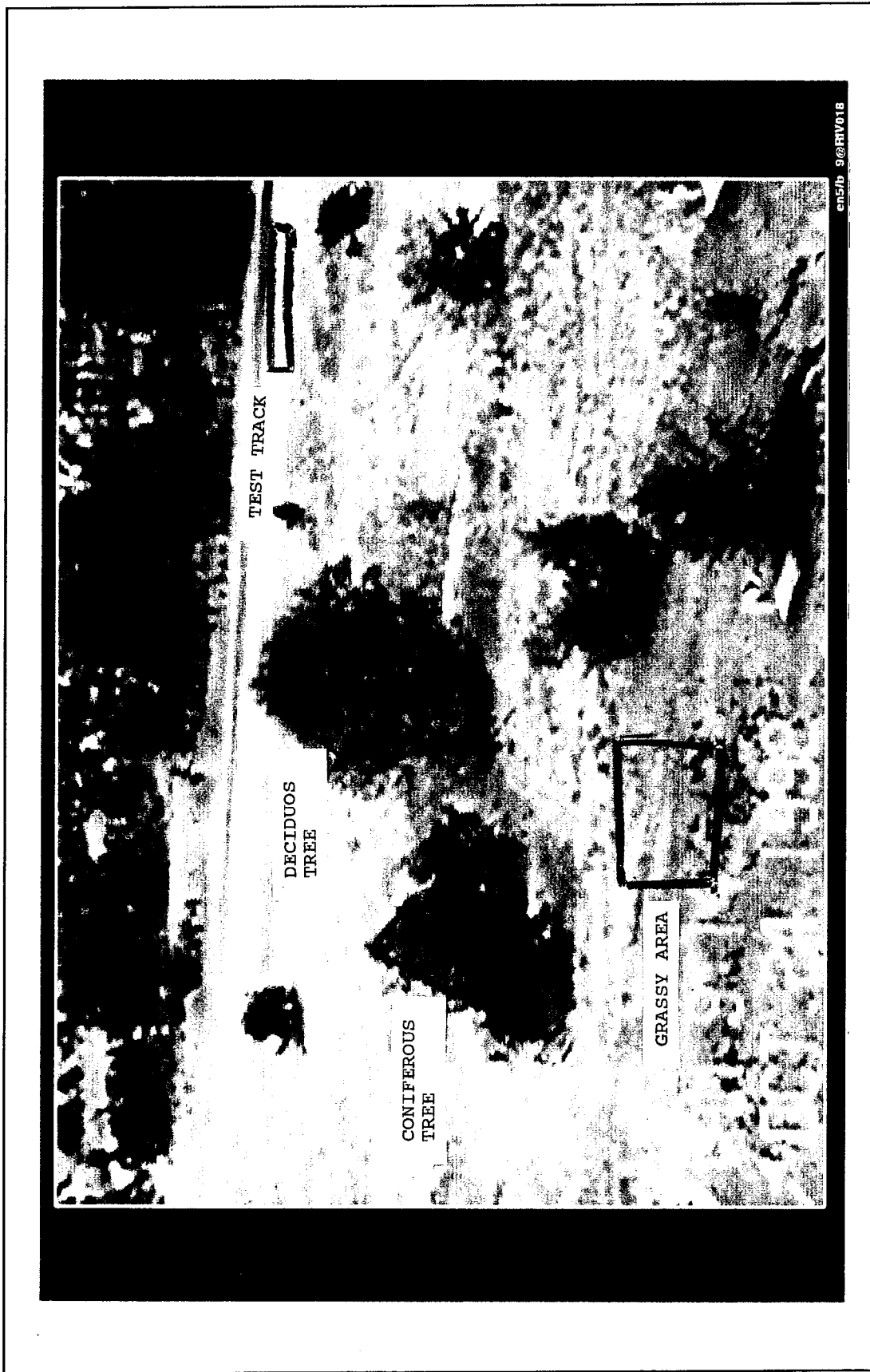


Figure 1. Photograph of Site E area

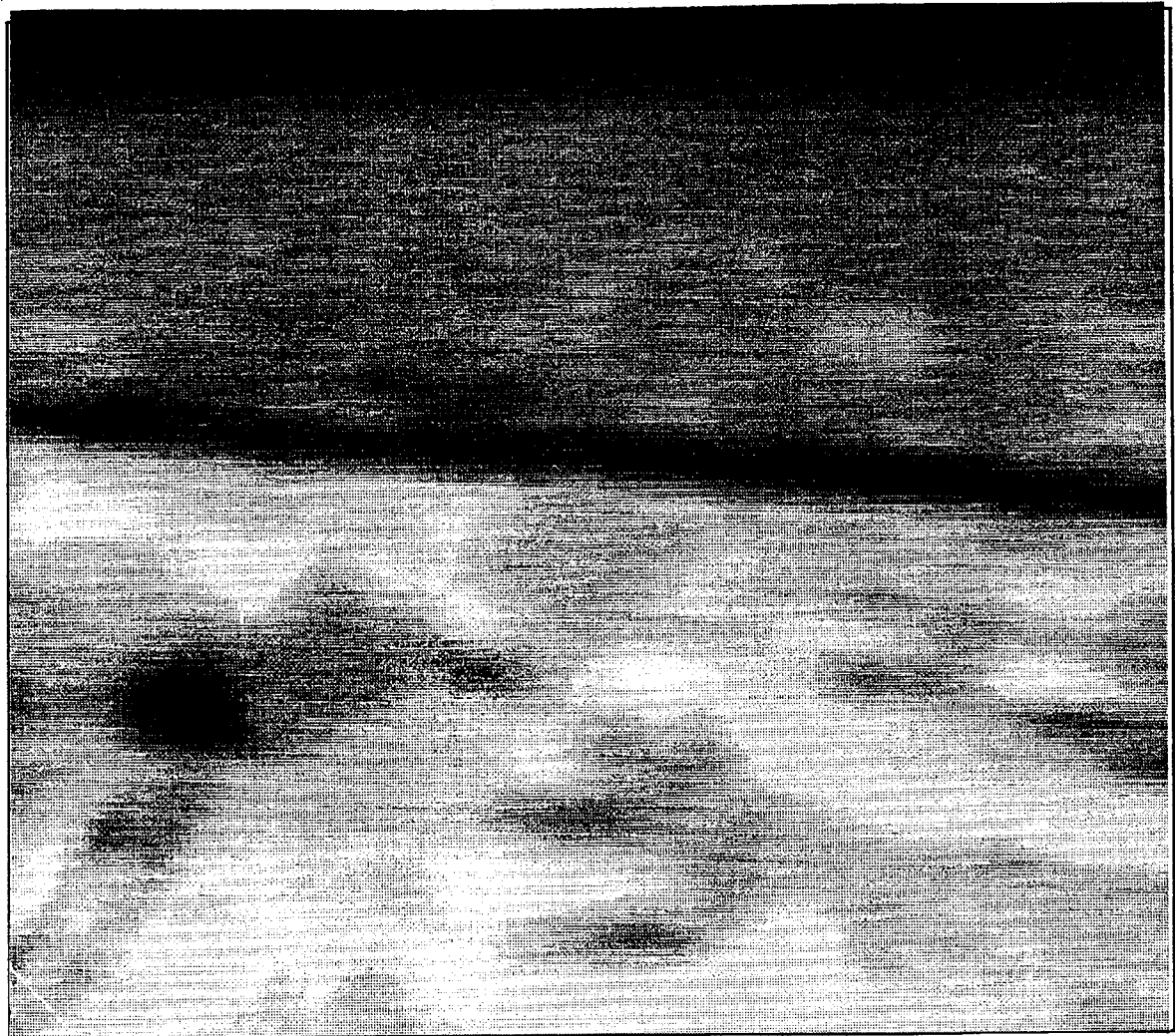


Figure 2. Sample of Site E area, LWB IR image (23OCT92:12:20)

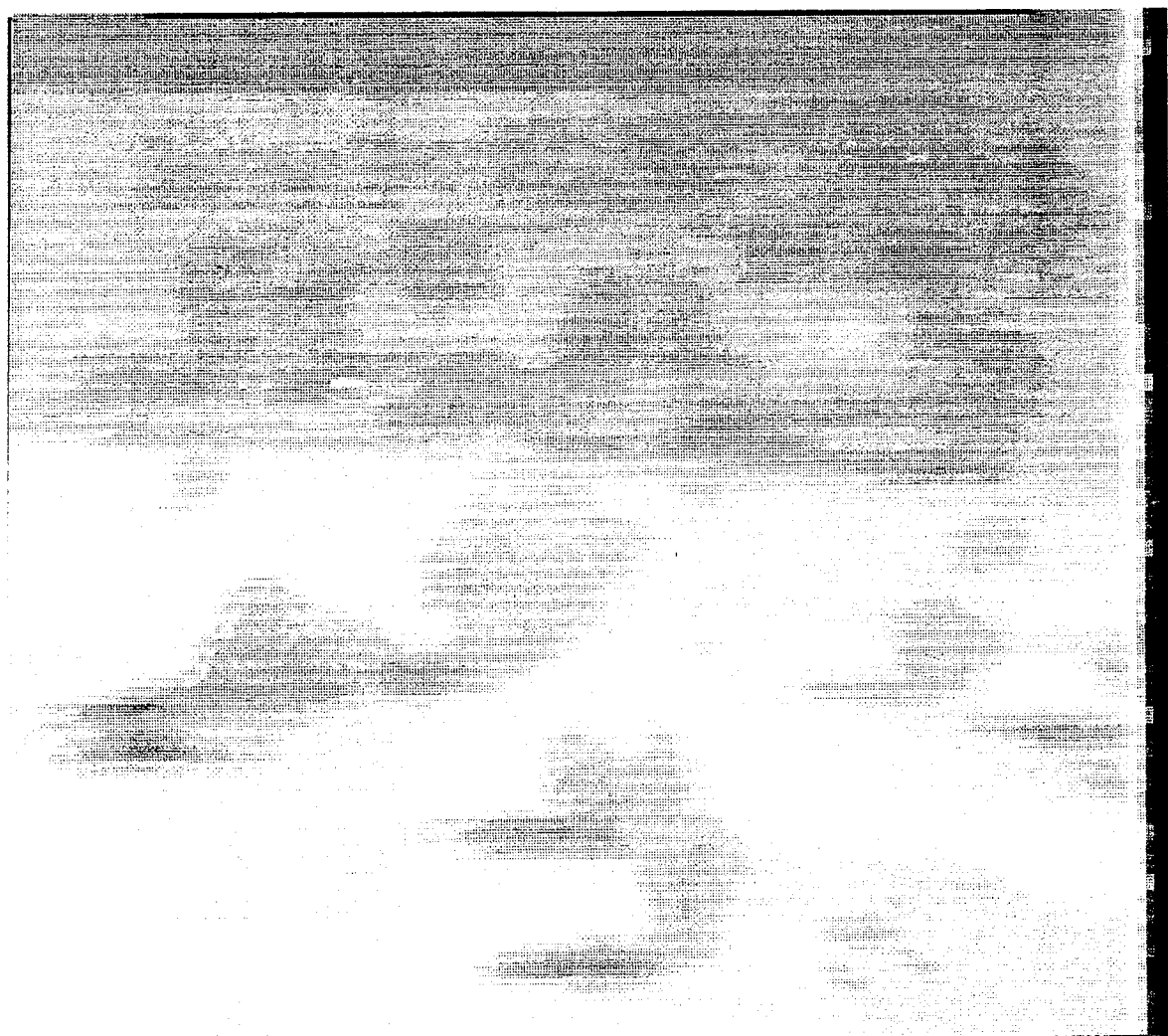


Figure 3. Sample of Site E area, SWB IR image (23OCT92:12:20)

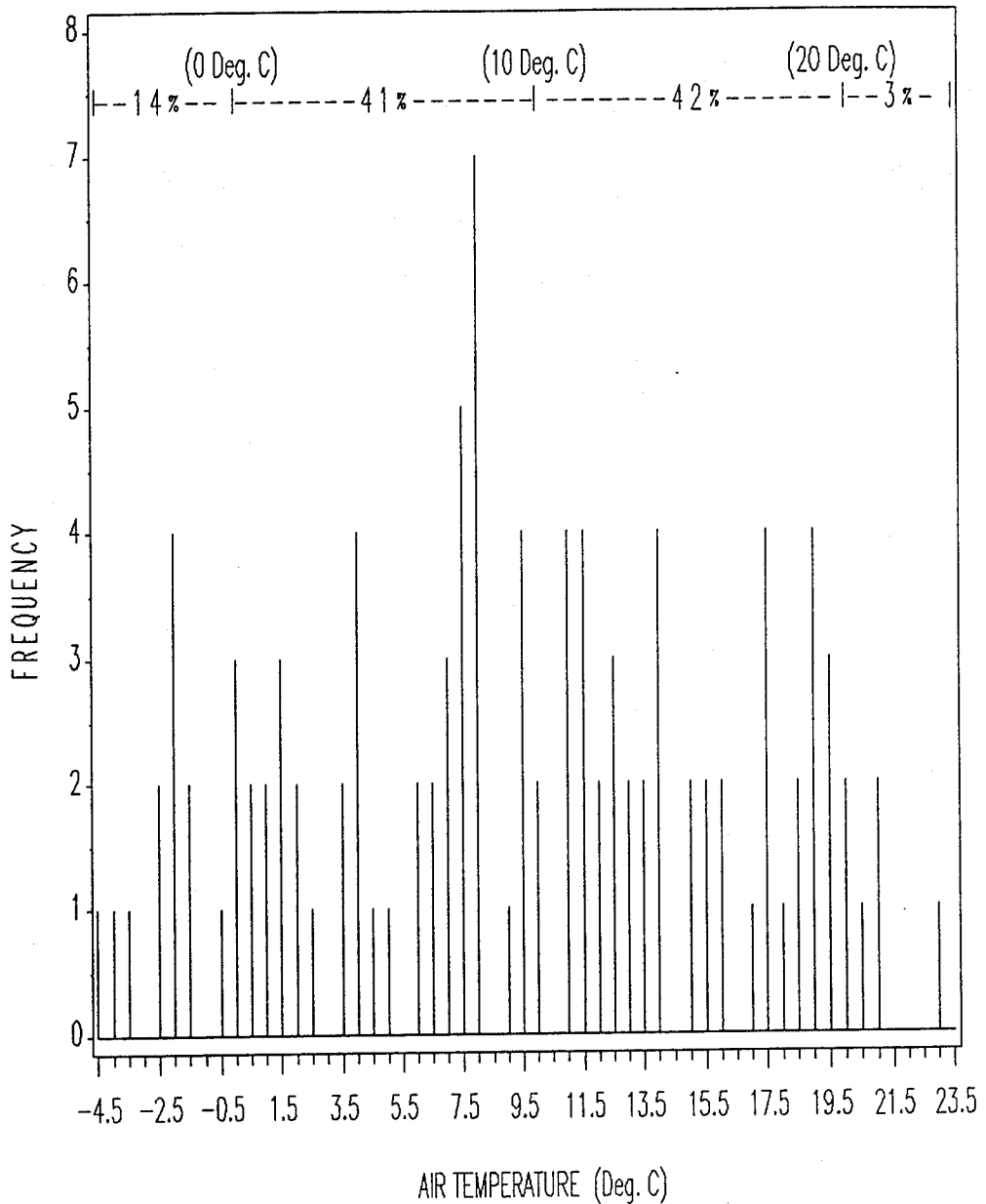


Figure 4. Histogram of air temperature distribution at critical frames

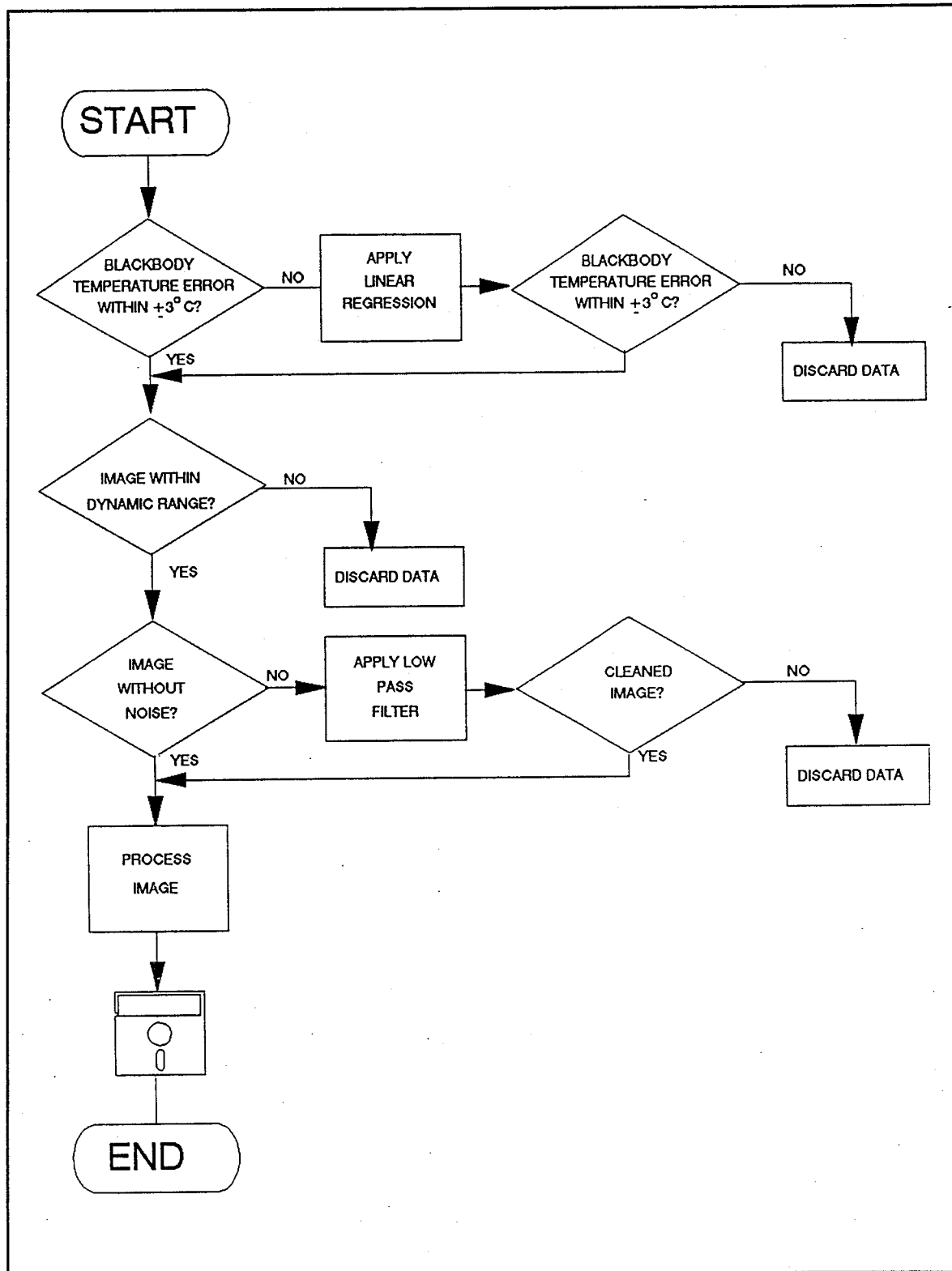


Figure 5. Imagery quality assurance procedure

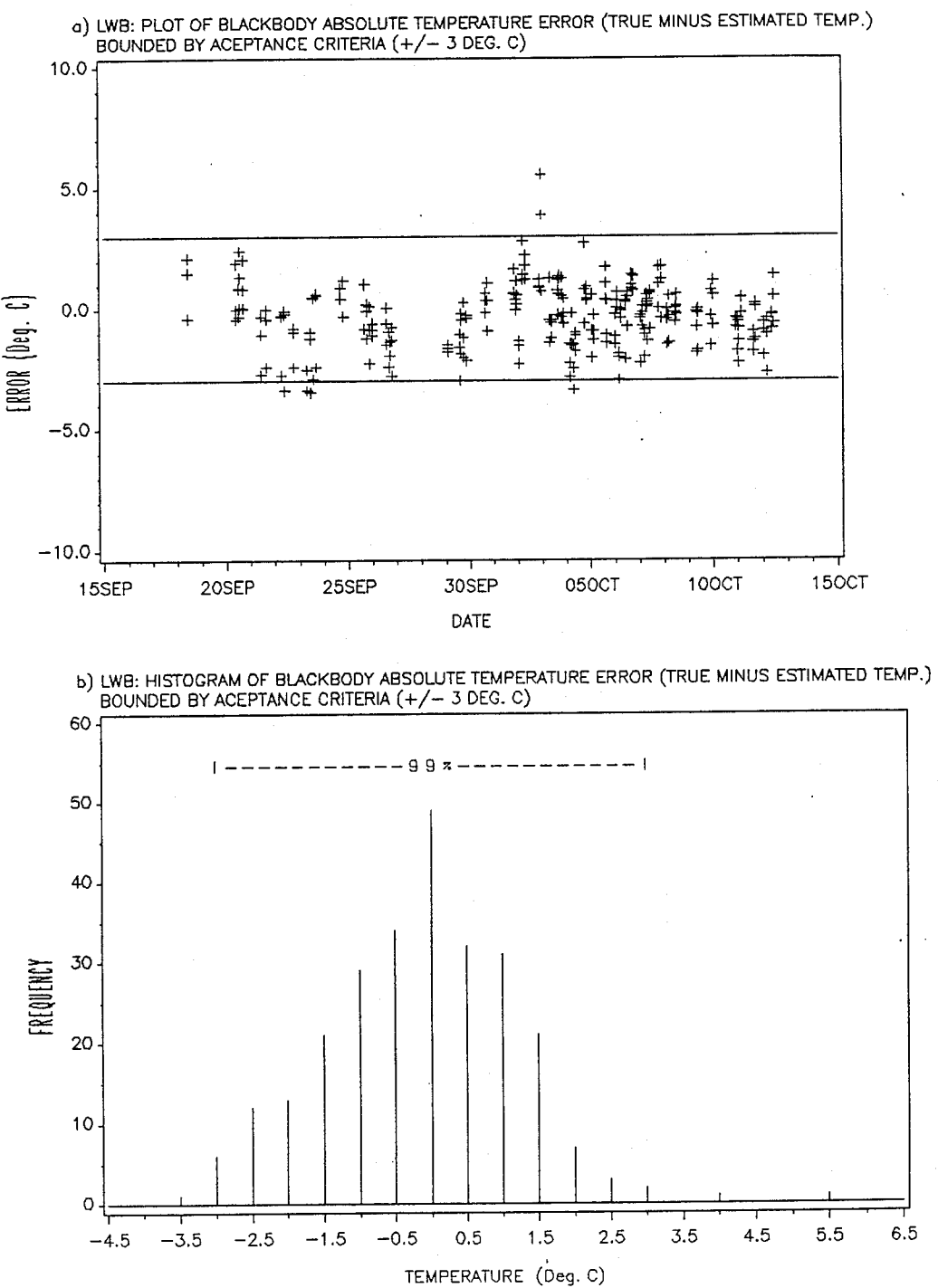


Figure 6. Blackbody calibration analysis for LWB data, no calibration correction needed

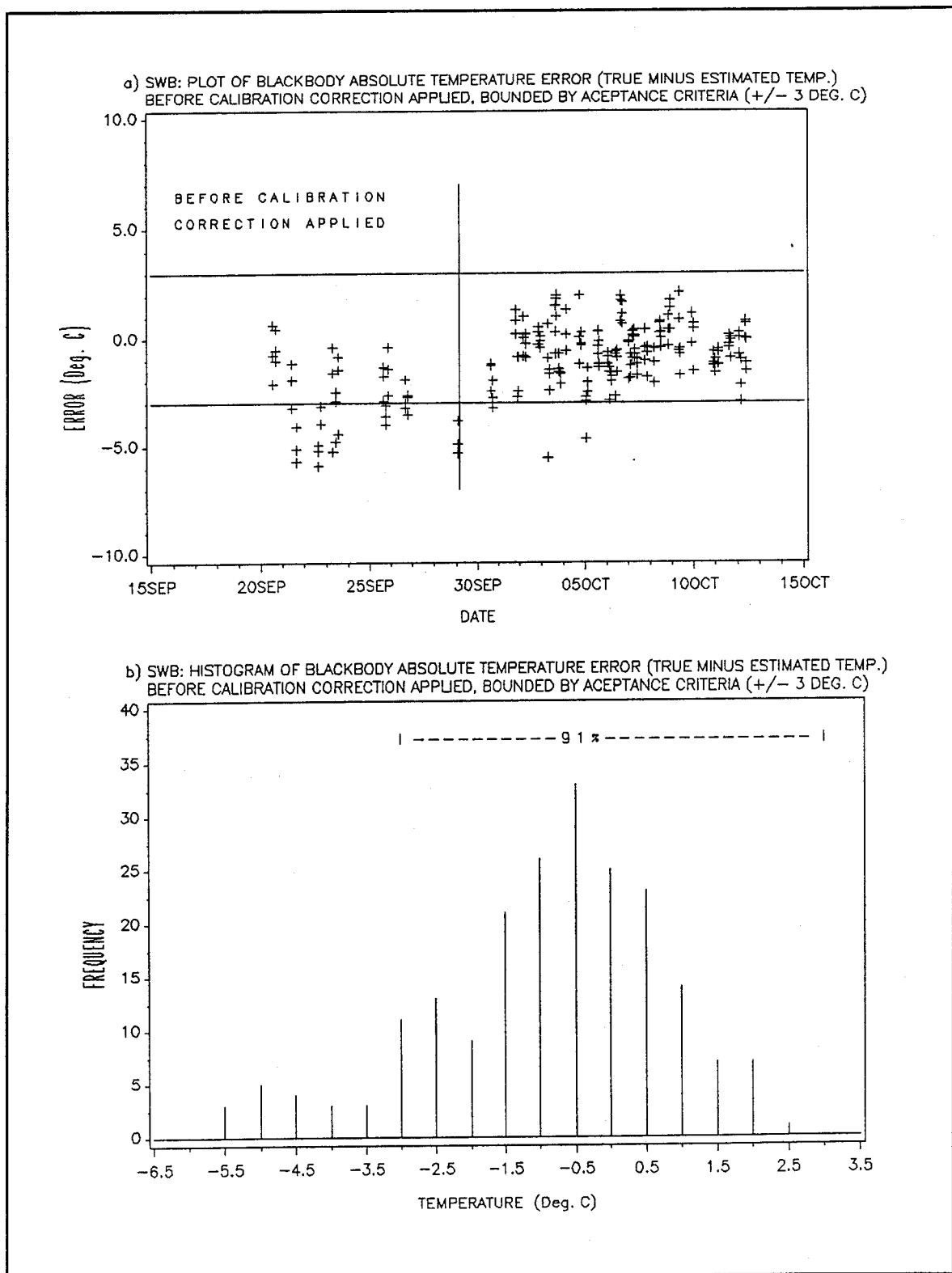


Figure 7. Blackbody calibration analysis before calibration correction applied to SWB data

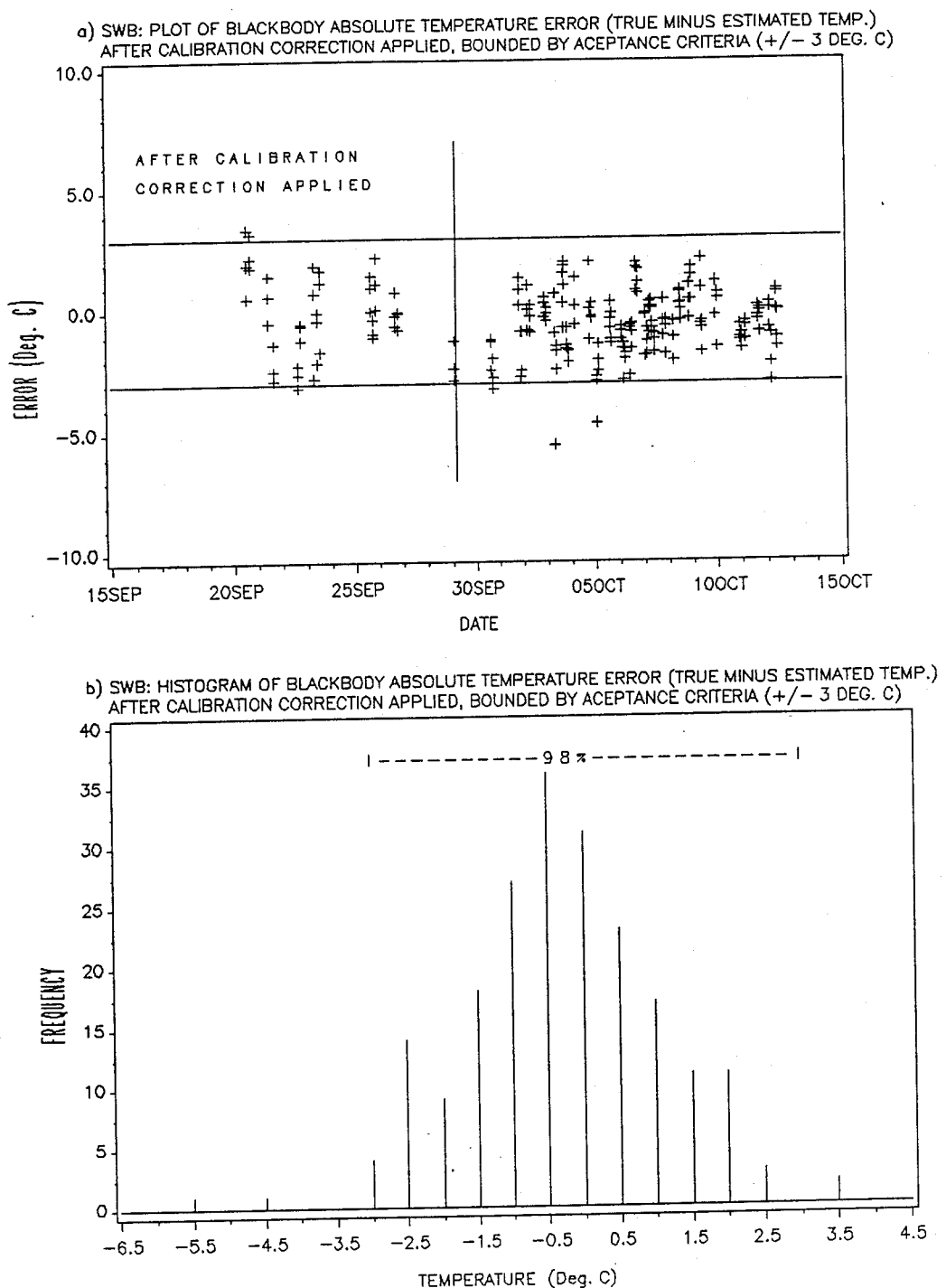


Figure 8. Blackbody calibration analysis after calibration correction applied to SWB data

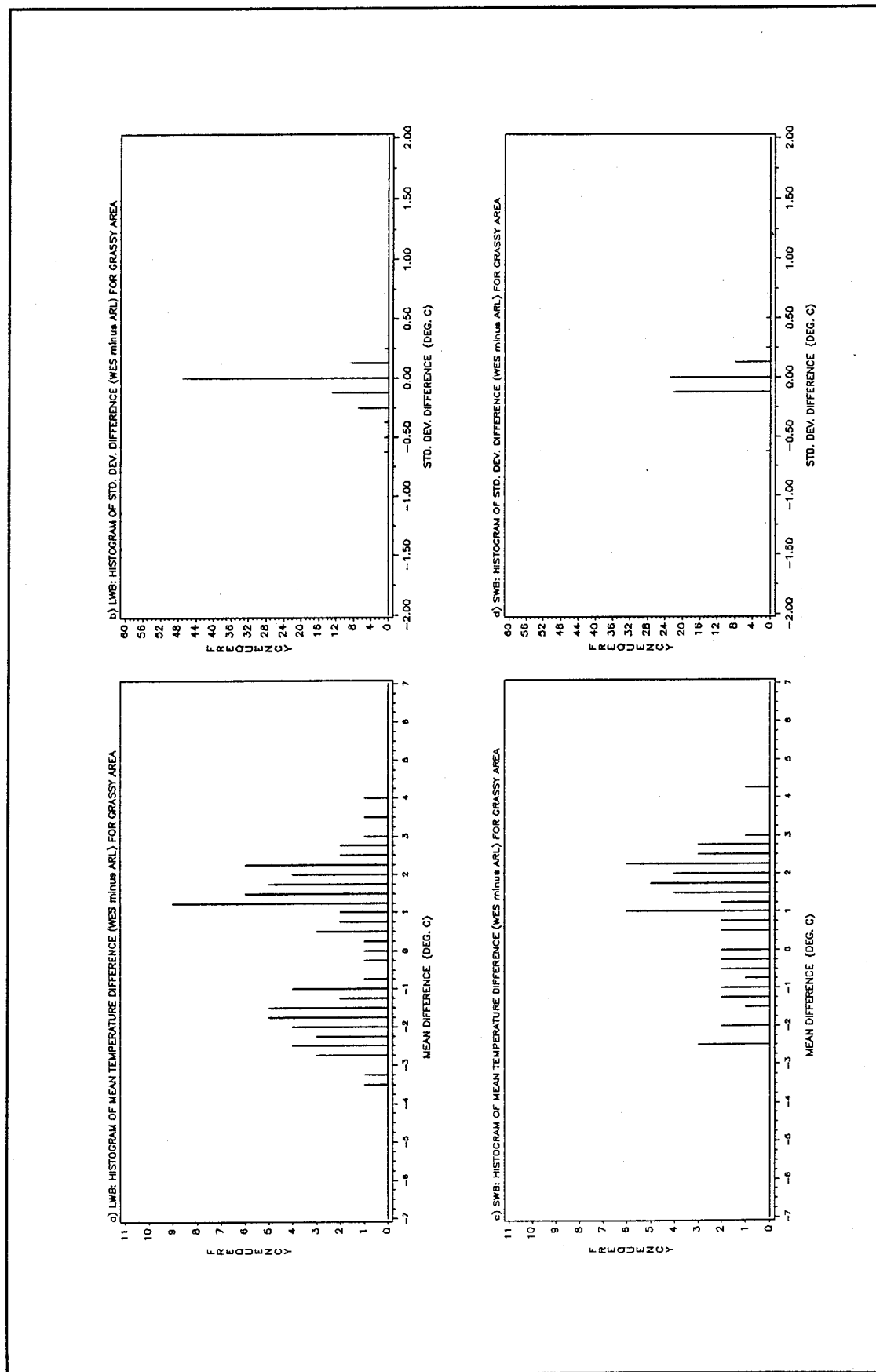


Figure 9. Sensor-to-sensor comparison between WES and ARL on grassy area feature for both wave bands

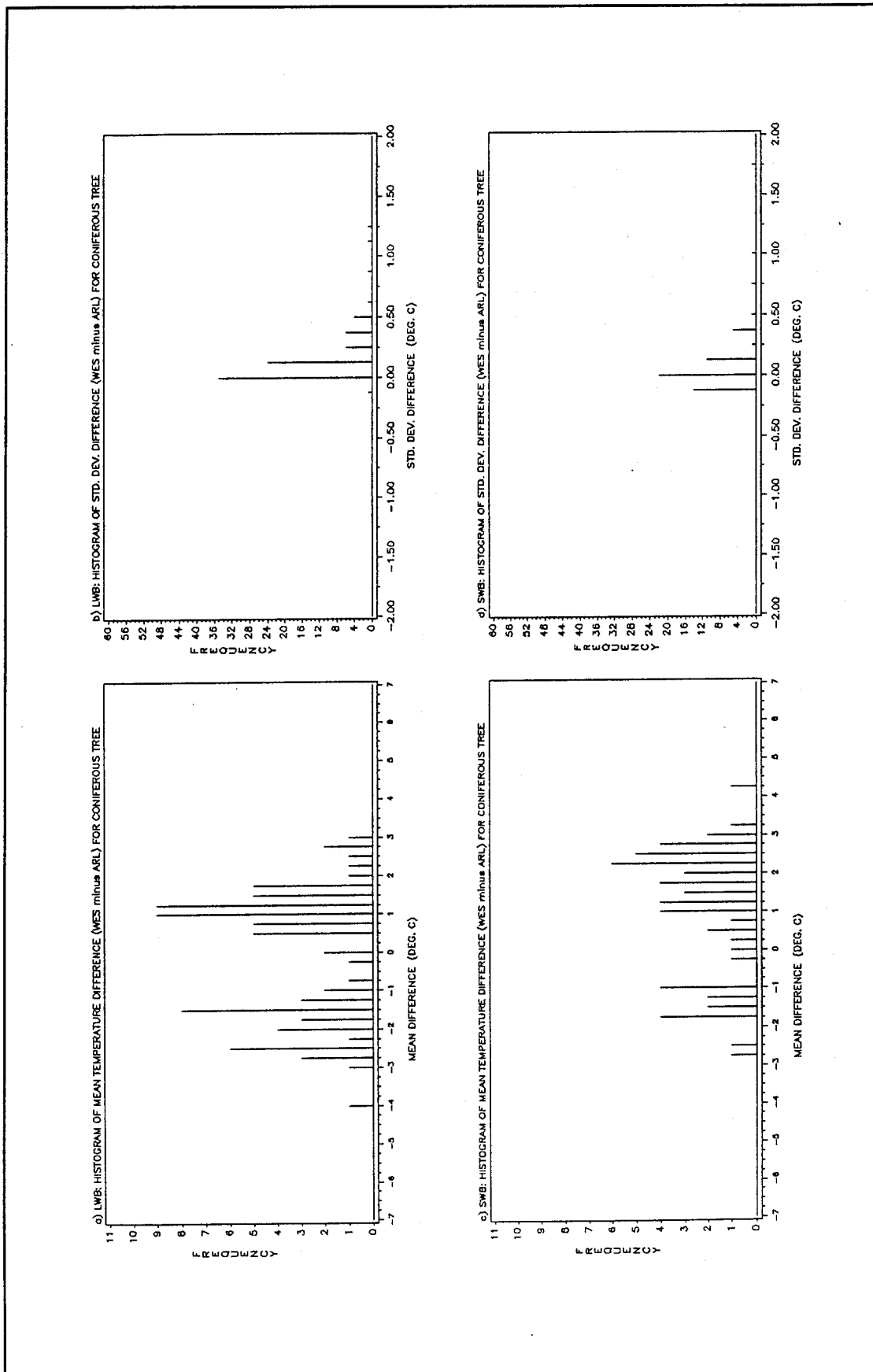


Figure 10. Sensor-to-sensor comparison between WES and ARL on coniferous tree feature for both wave bands

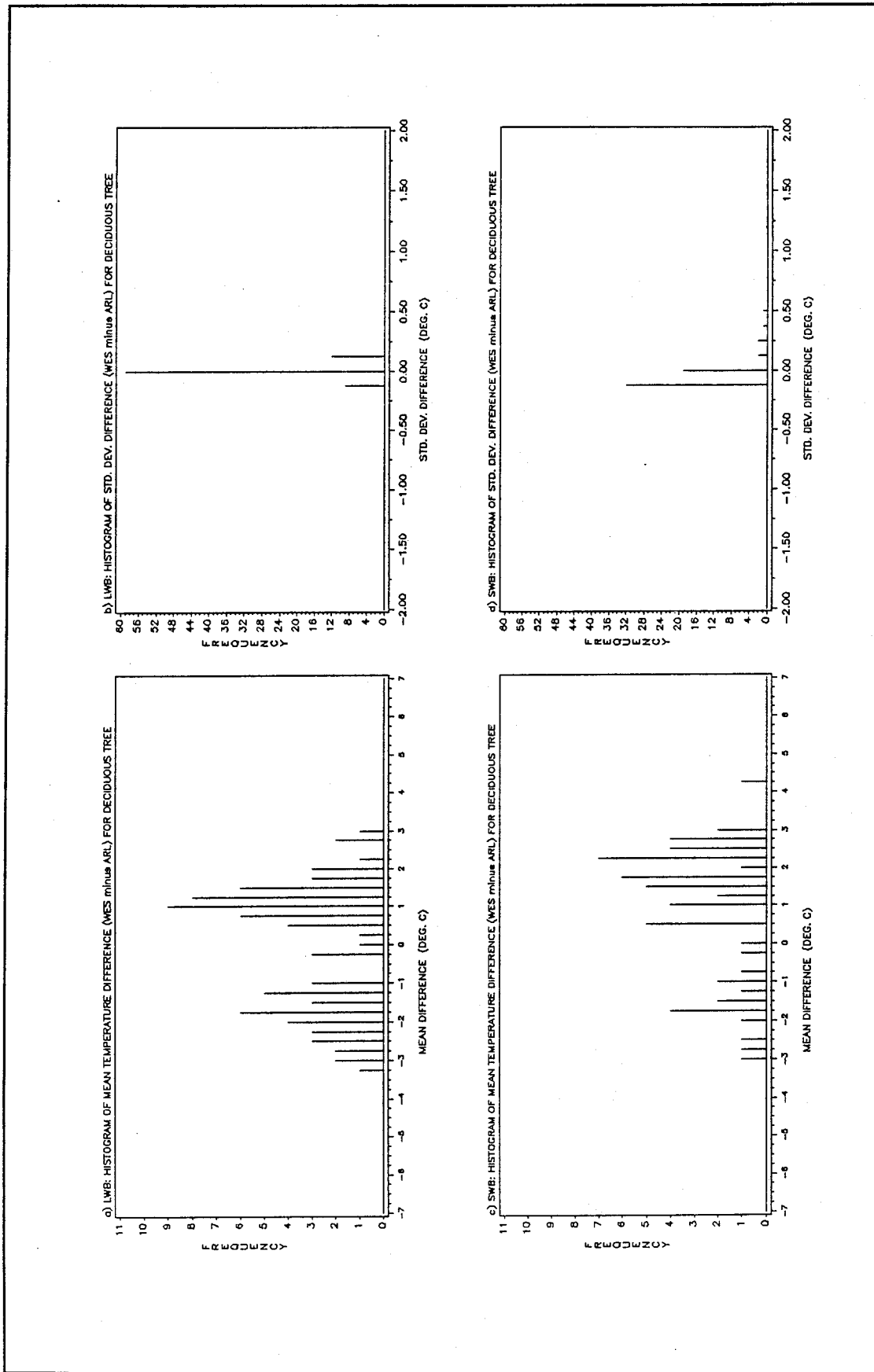


Figure 11. Sensor-to-sensor comparison between WES and ARL on deciduous tree feature for both wave bands

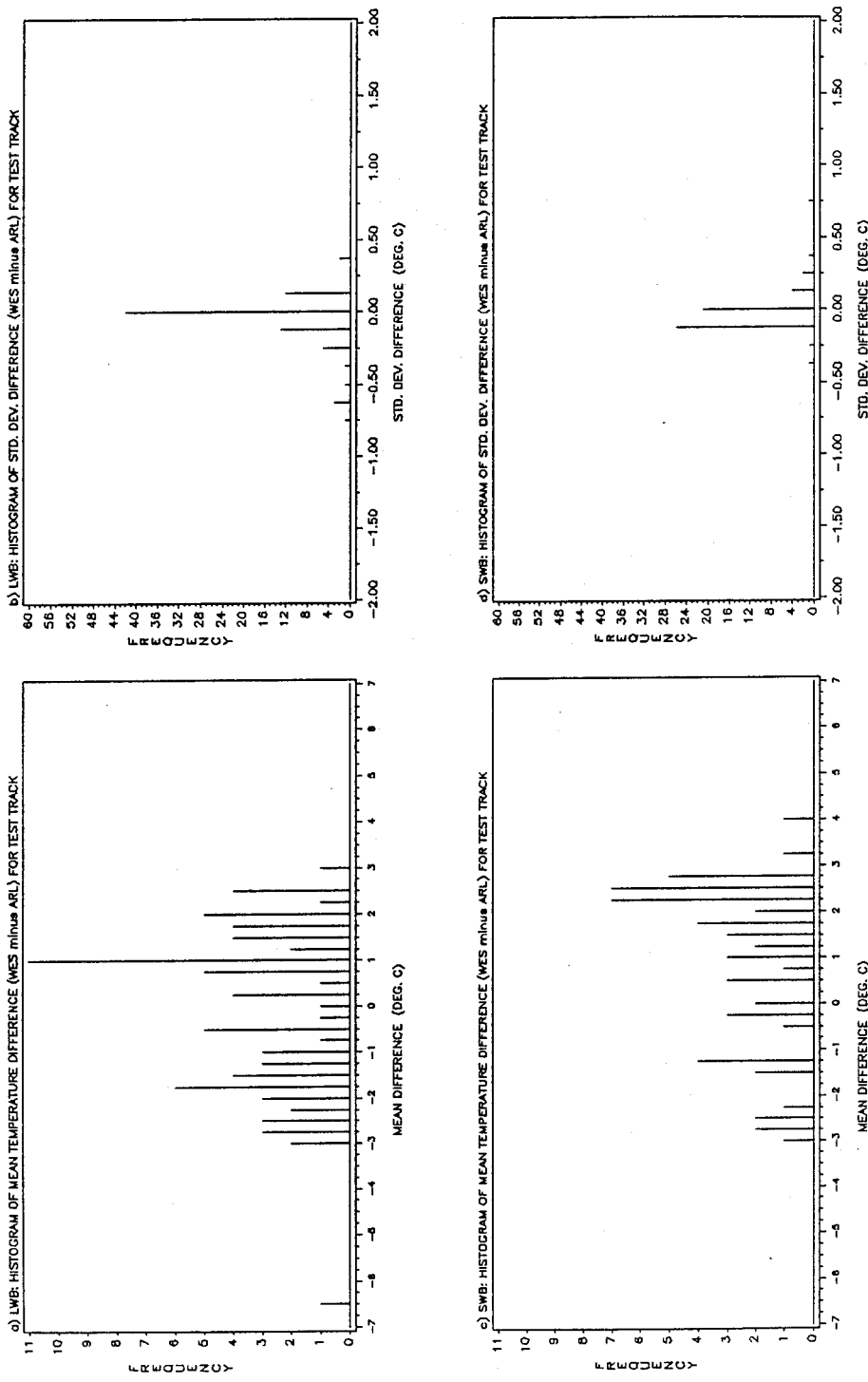


Figure 12. Sensor-to-sensor comparison between WES and ARL on test track feature for both wave bands

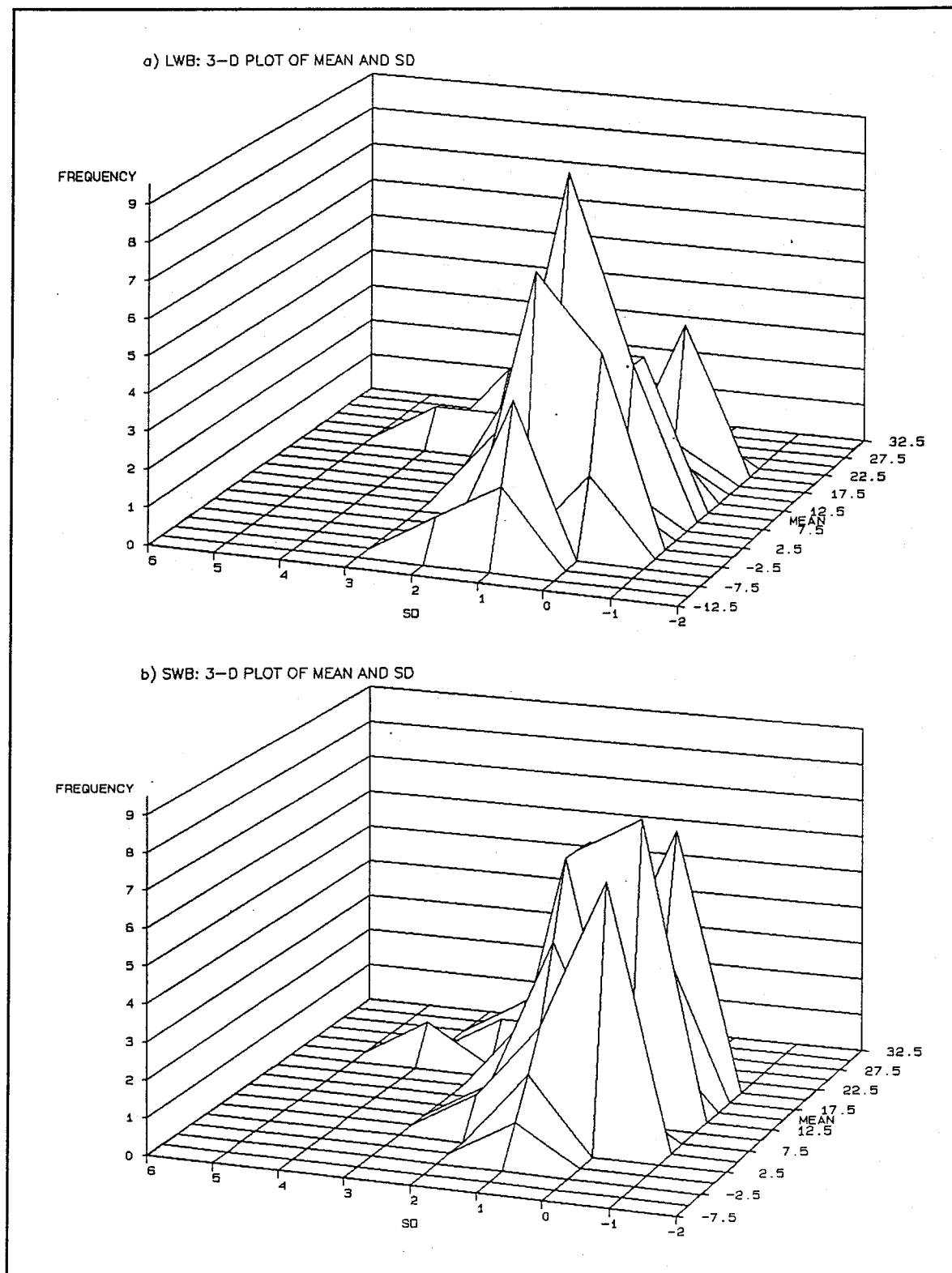


Figure 13. 3-D plot of image mean temperature and standard deviation distribution for both wave bands

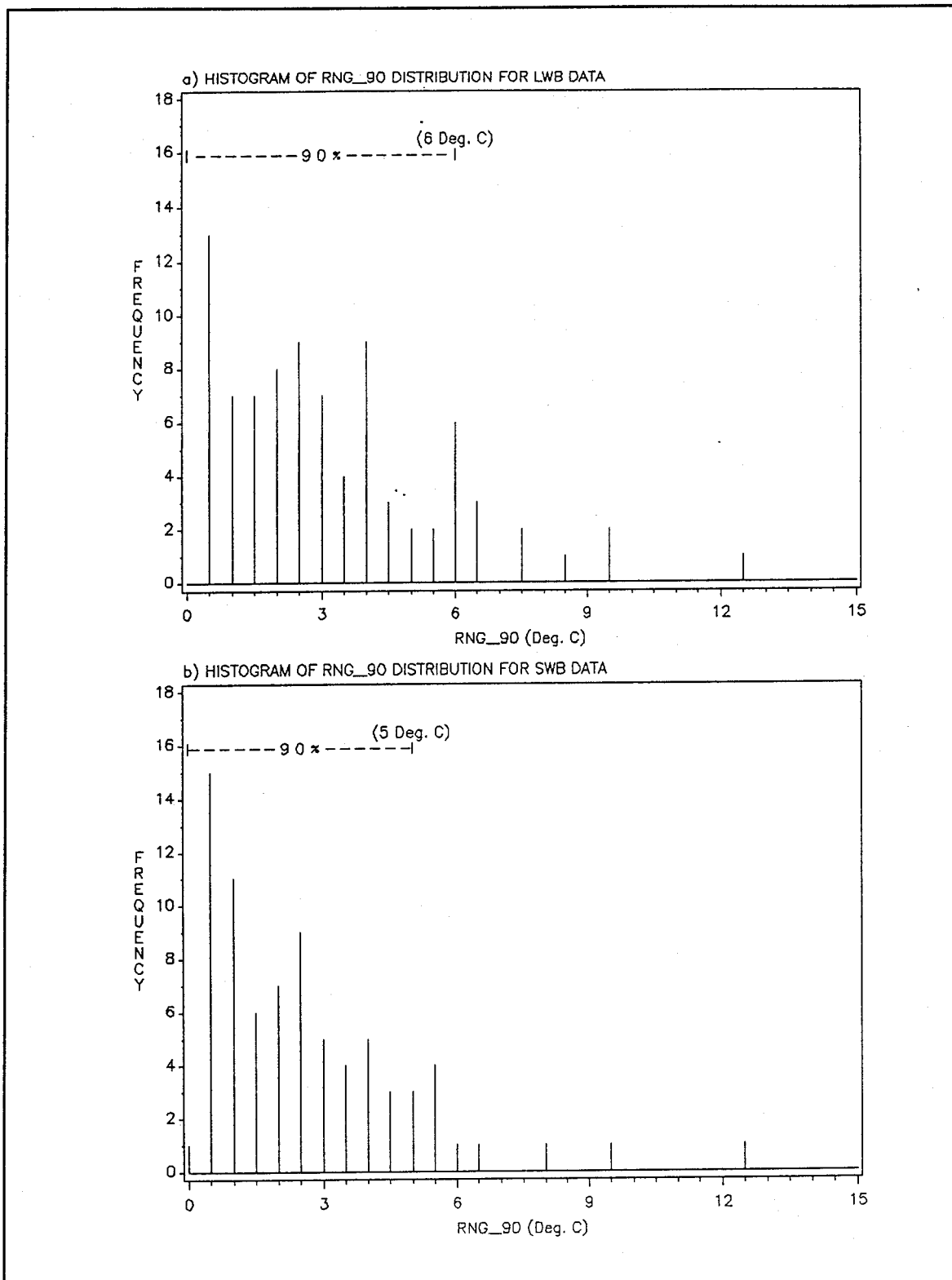


Figure 14. Histogram plot of temperature range distribution for LWB and SWB data

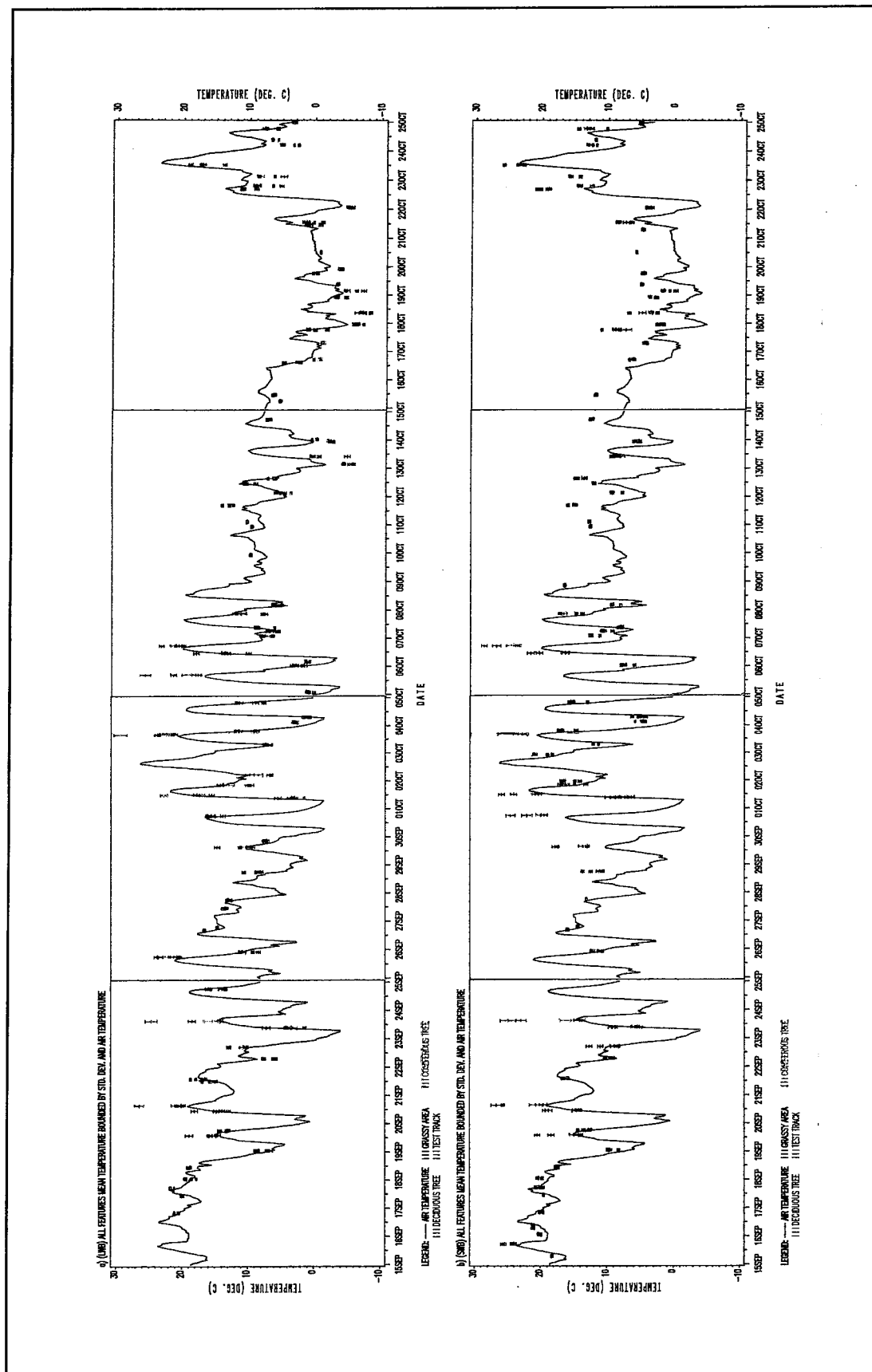


Figure 15. Air temperature and features' mean temperature bounded by standard deviation throughout Grayling 1 test

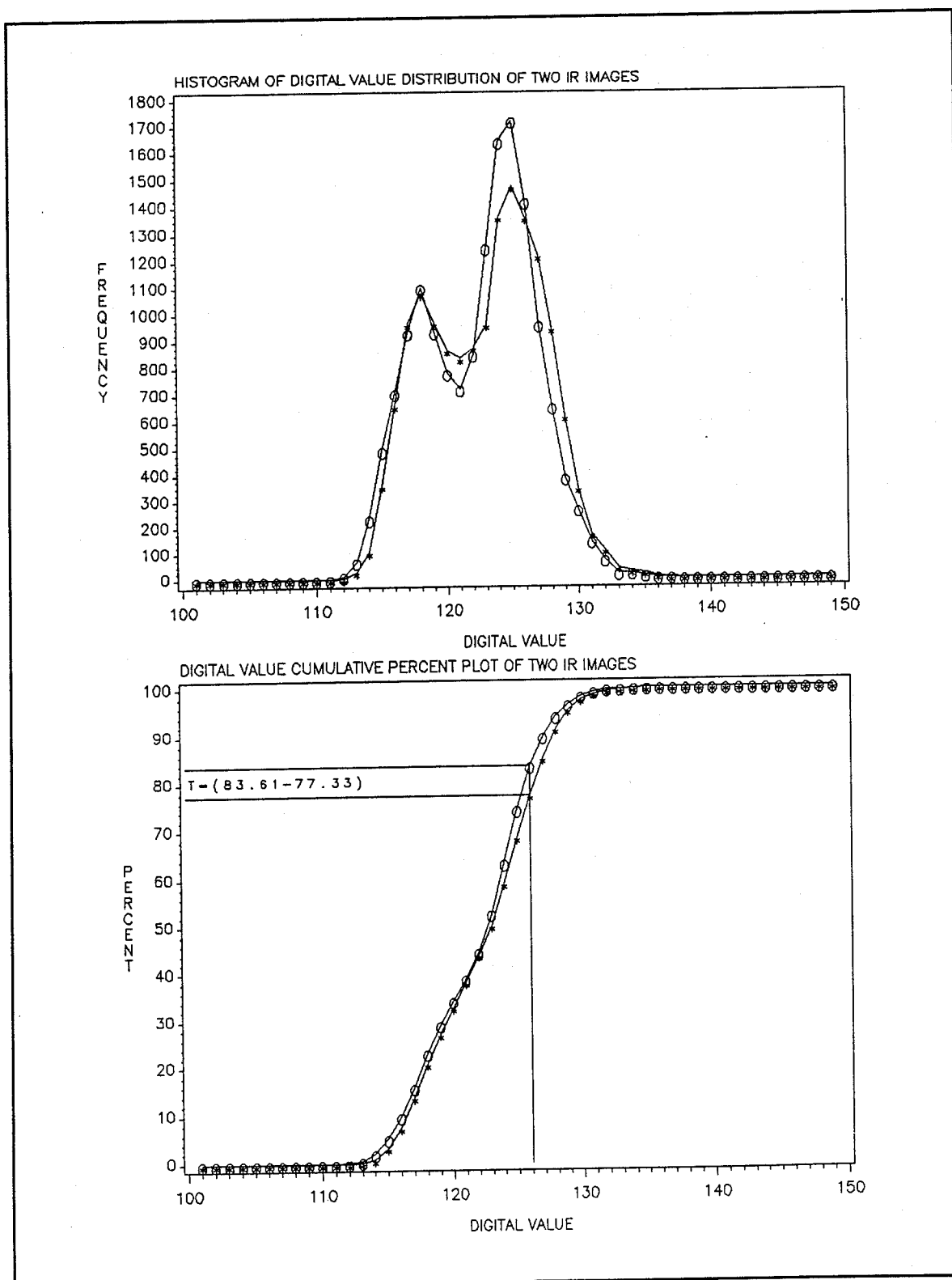


Figure 16. Within pass analysis plot

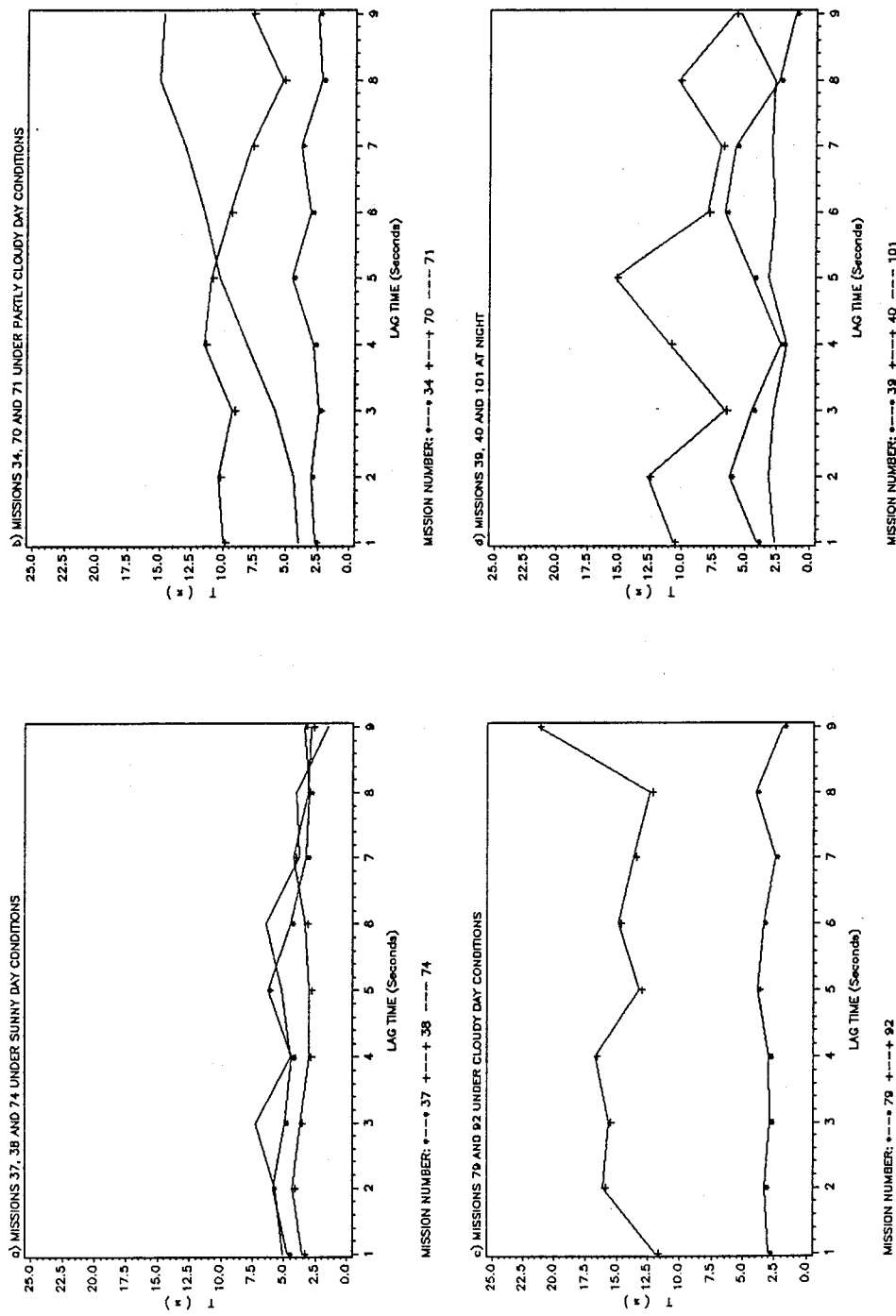


Figure 17. Plot of T versus lag time at different weather conditions for LWB data

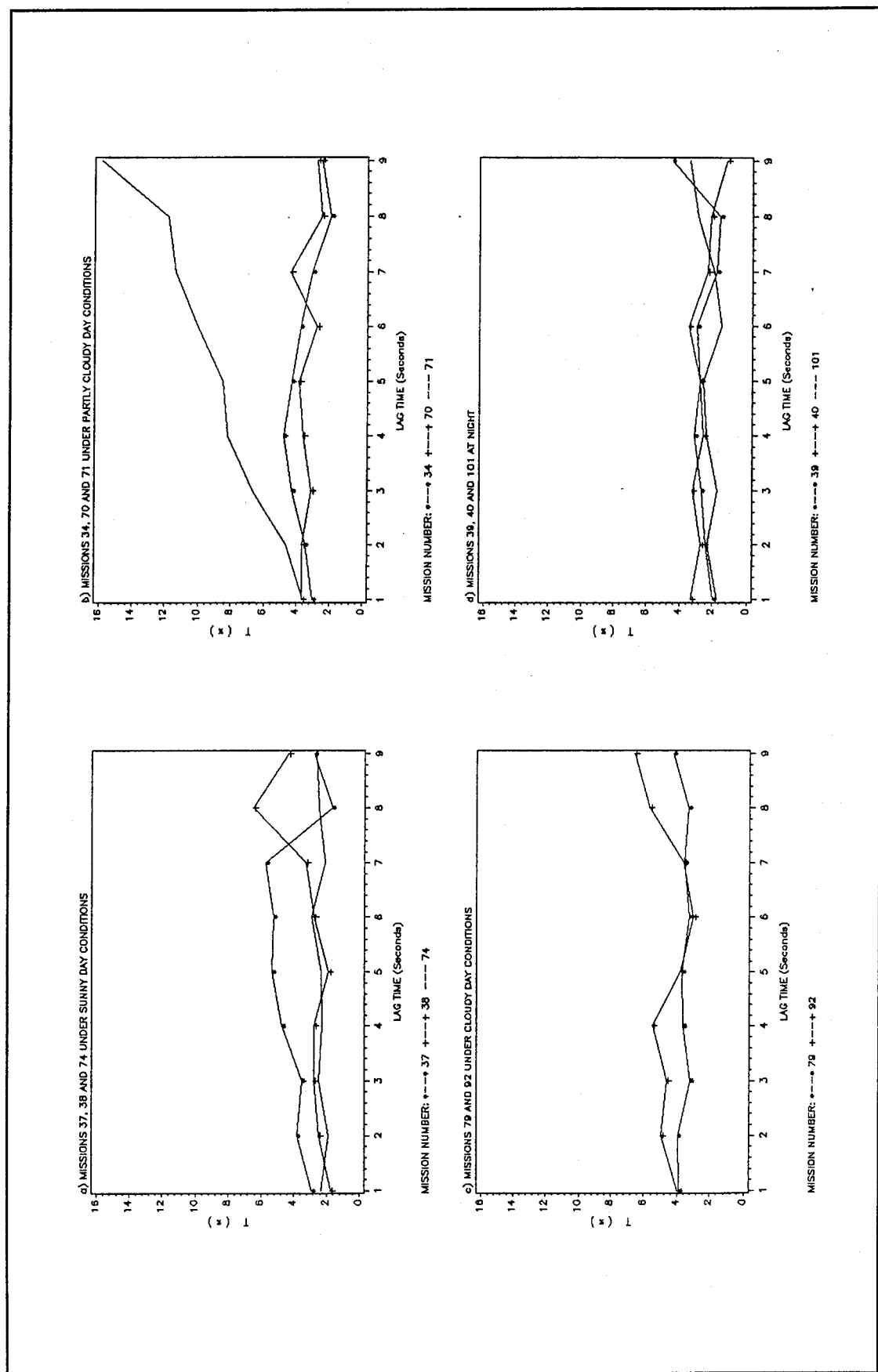


Figure 18. Plot of T versus lag time at different weather conditions for SWB data

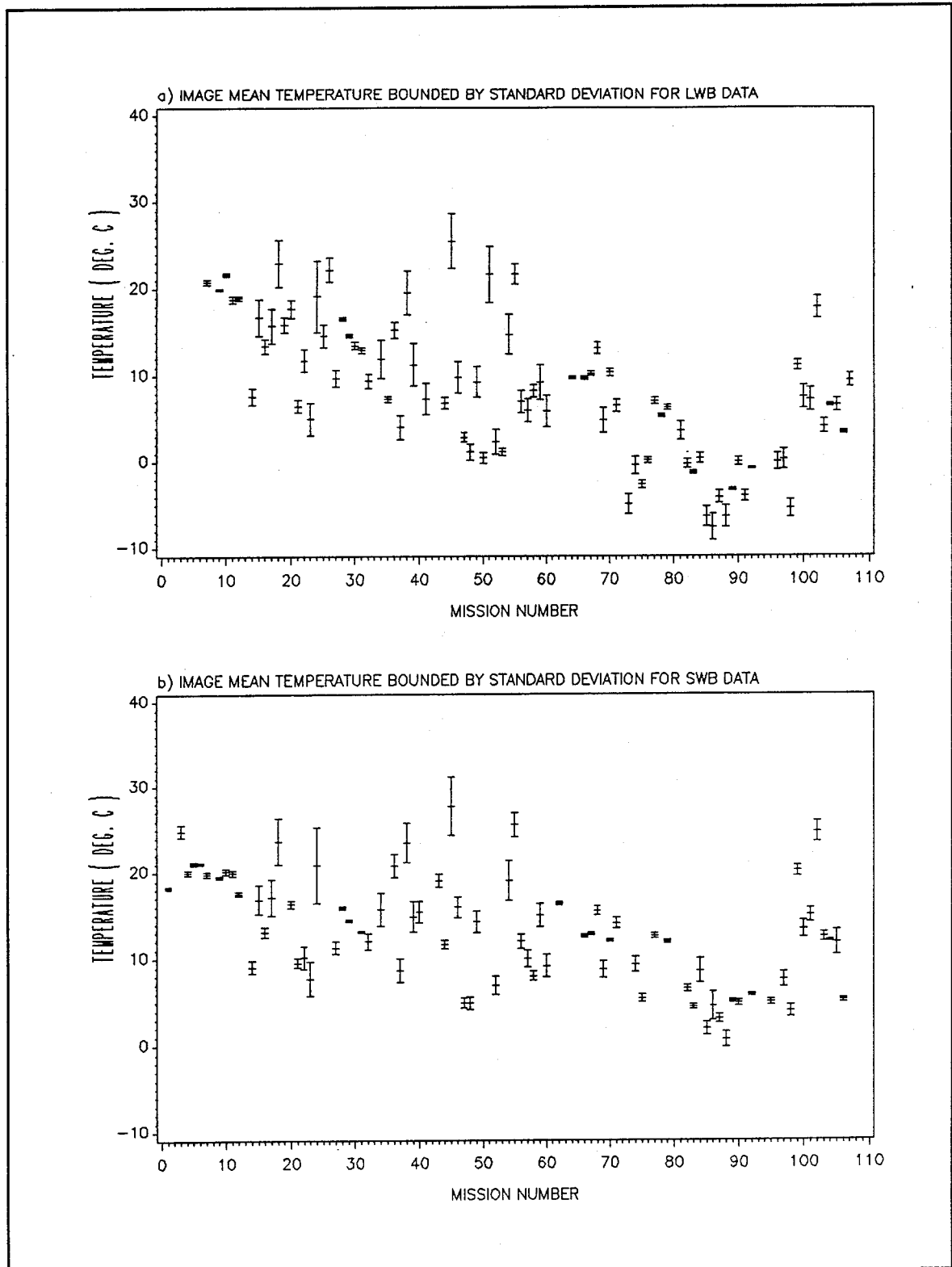


Figure 19. Image mean temperature bounded by standard deviation for LWB and SWB data for all 107 missions

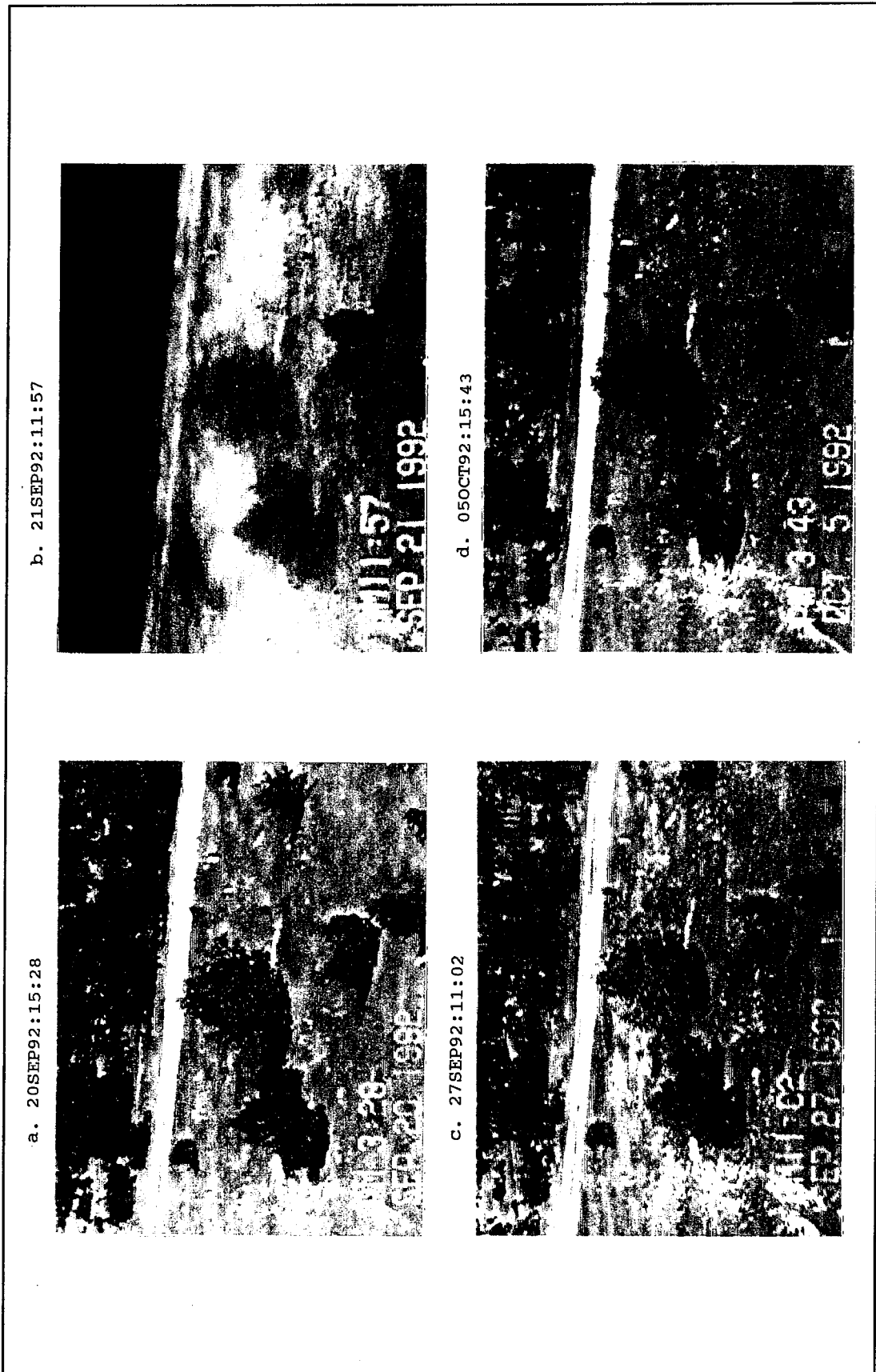


Figure 20. Physical changes at Site E area (Sheet 1 of 3)

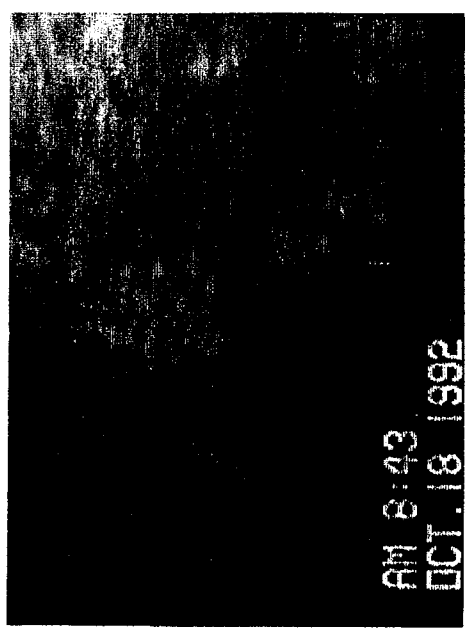
e. 12OCT92:10:48



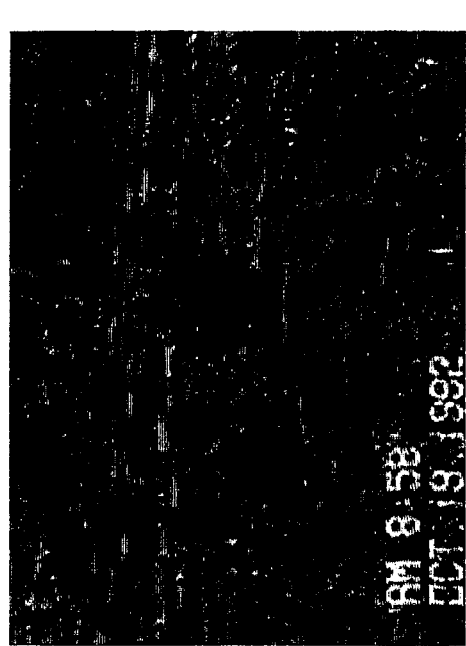
f. 17OCT92:17:54



g. 18OCT92:08:43



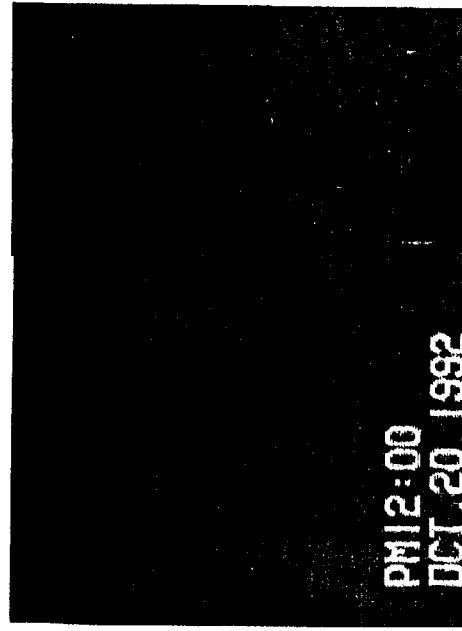
h. 19OCT92:08:58



i. 19OCT92:17:58



j. 20OCT92:12:00



k. 21OCT92:11:34



l. 22OCT92:16:19



Figure 20. (Sheet 3 of 3)

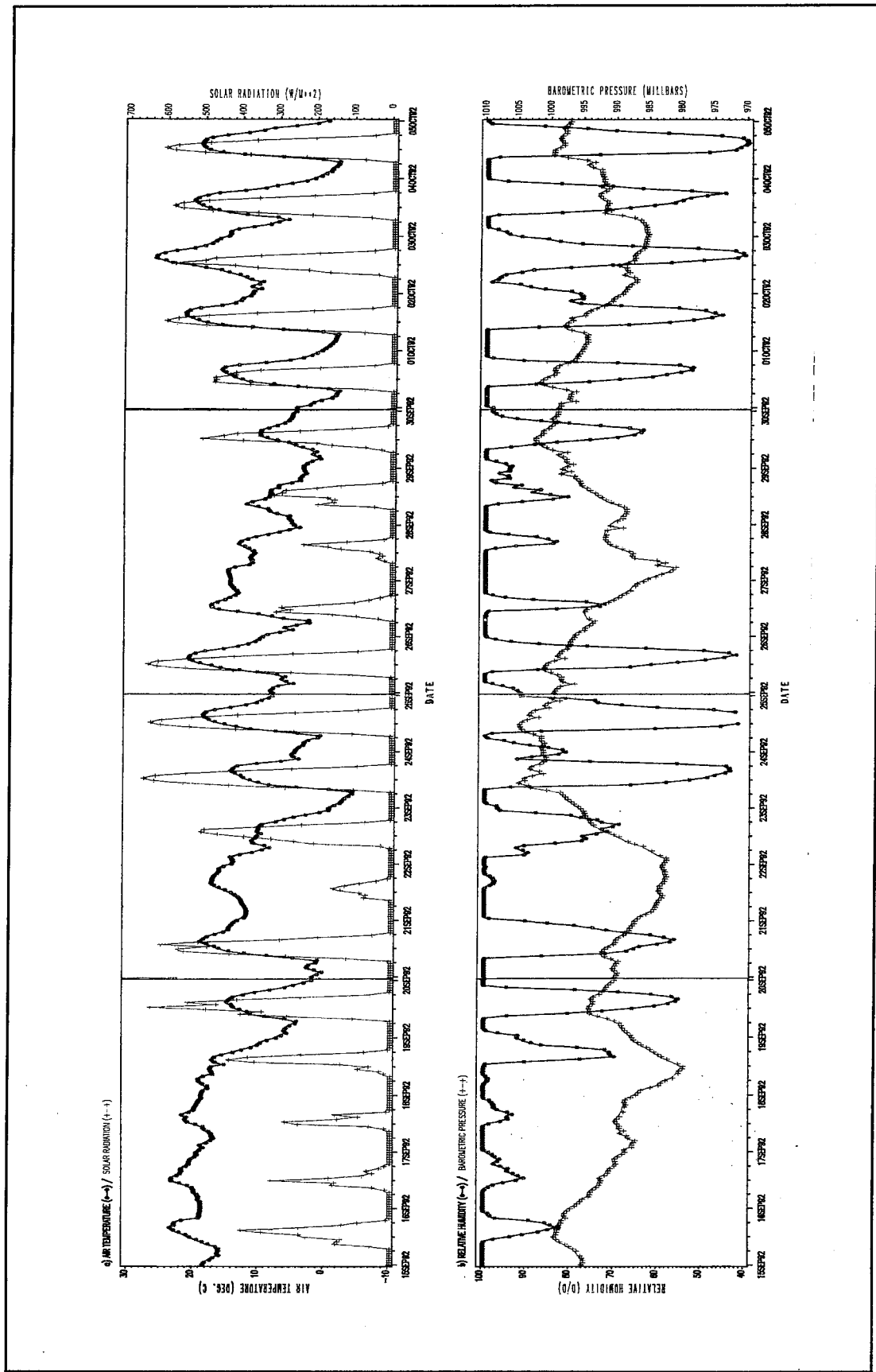


Figure 21. WES meteorological data throughout Grayling 1 test (Sheet 1 of 4)

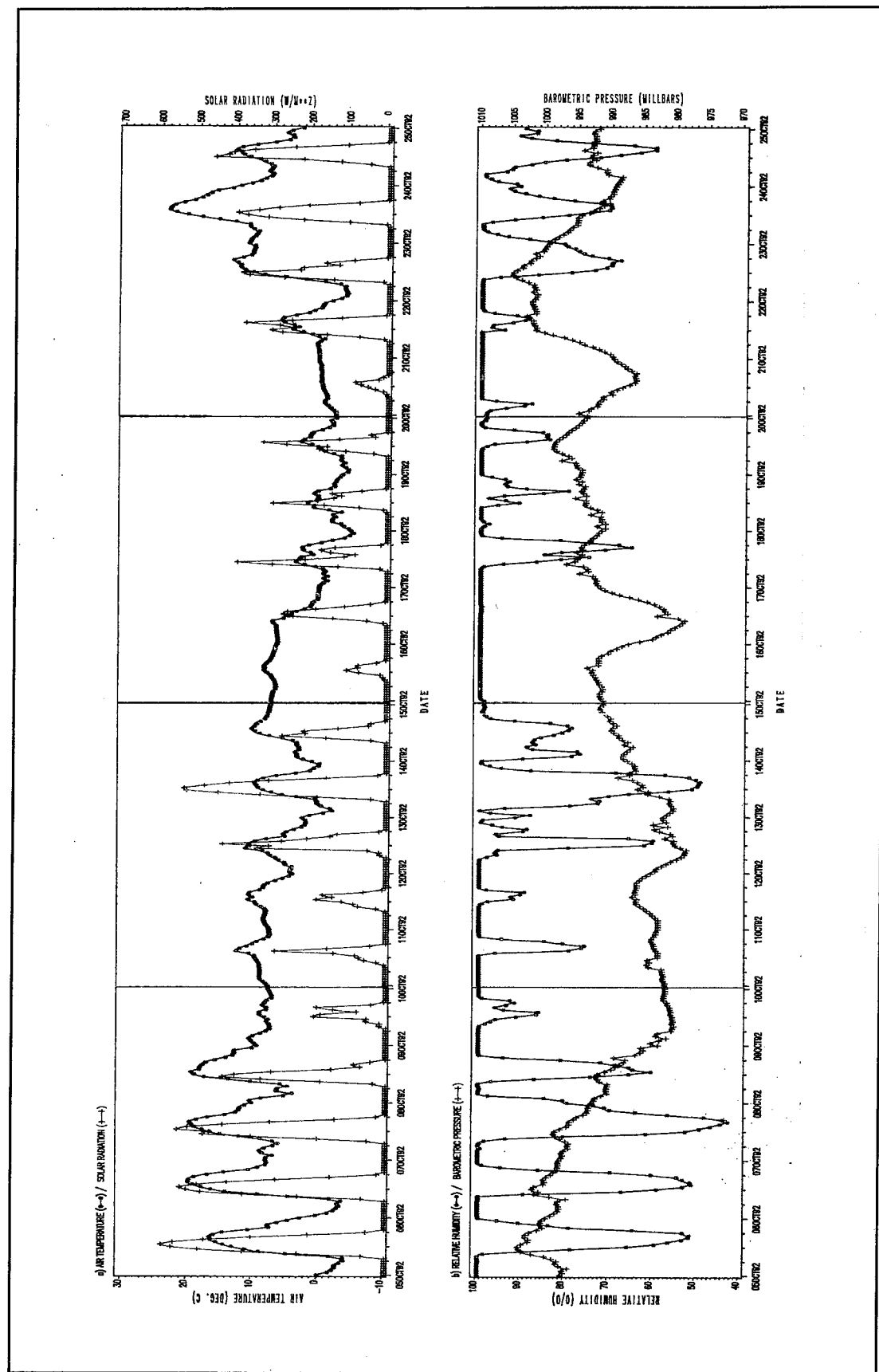


Figure 21. (Sheet 2 of 4)

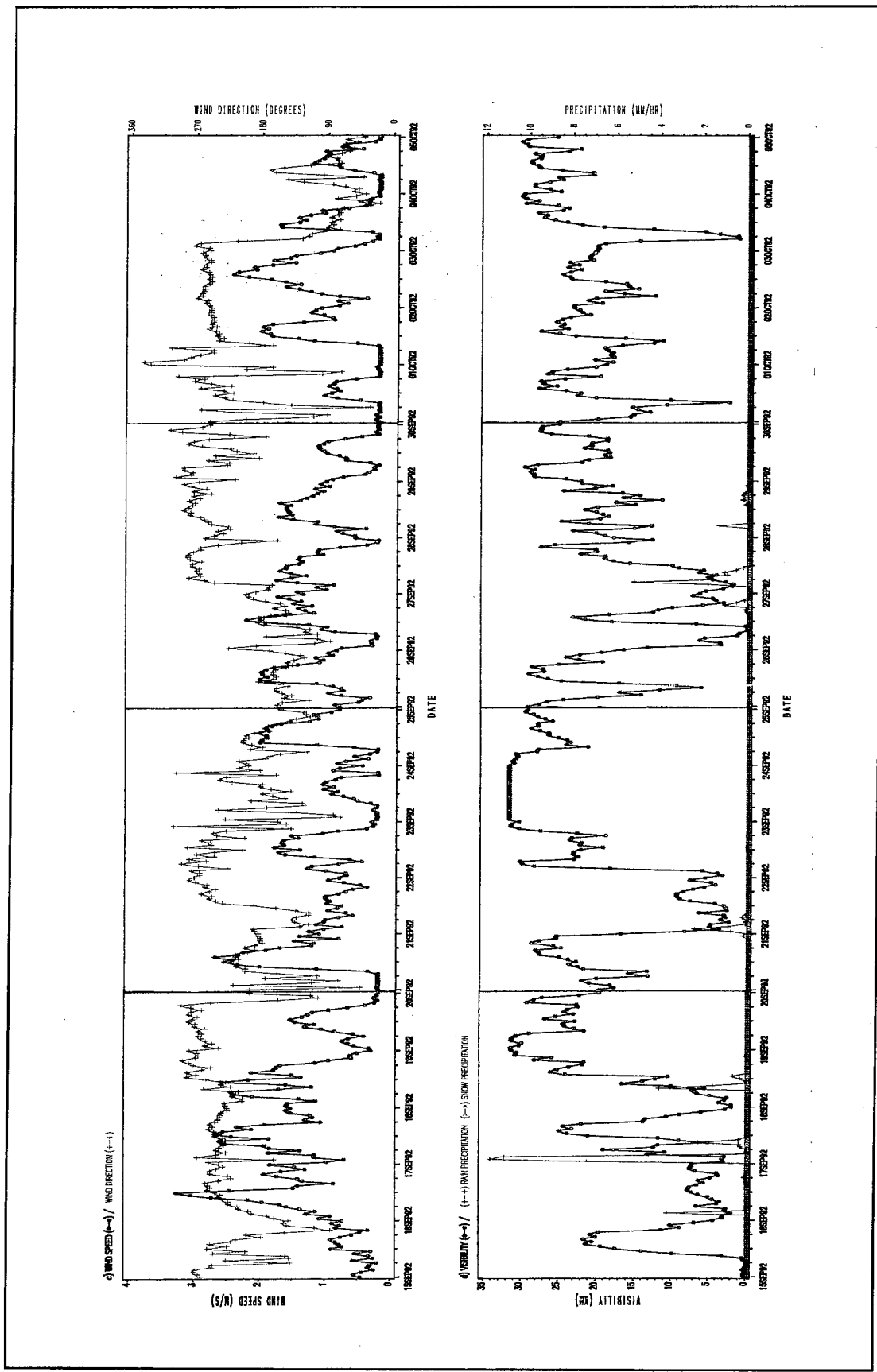


Figure 21. (Sheet 3 of 4)

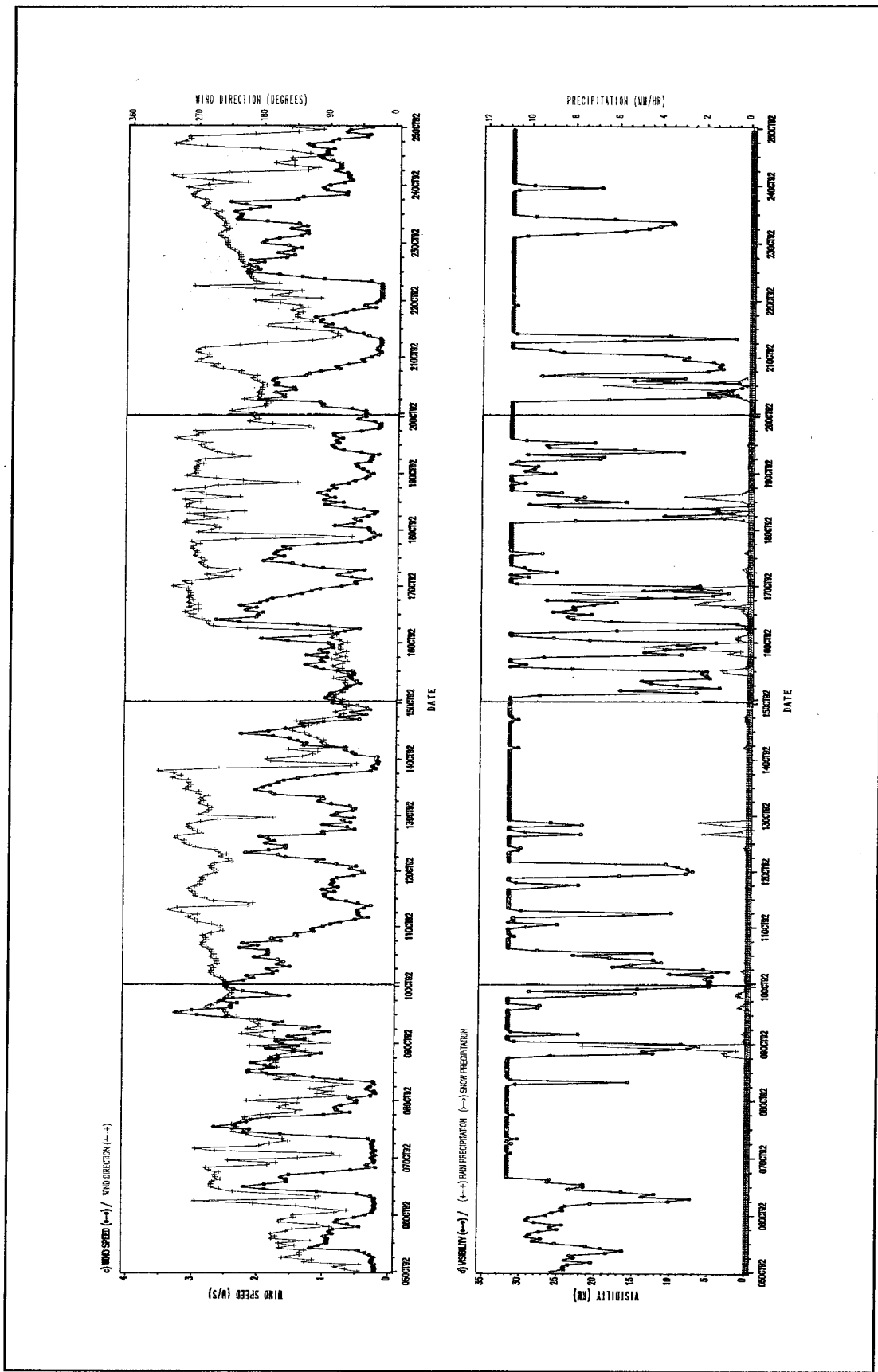


Figure 21. (Sheet 4 of 4)

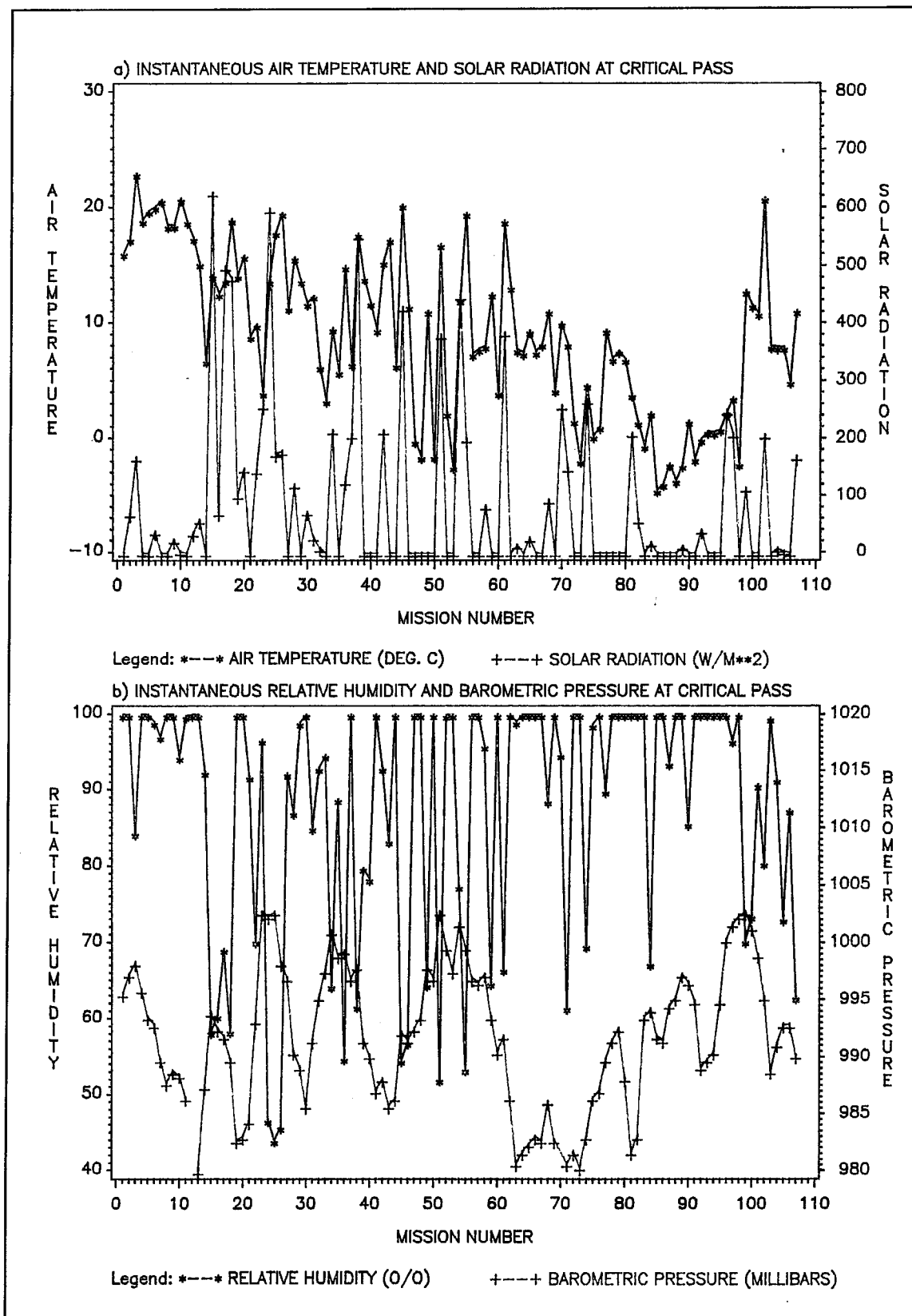


Figure 22. Instantaneous meteorological conditions at critical frames (Continued)

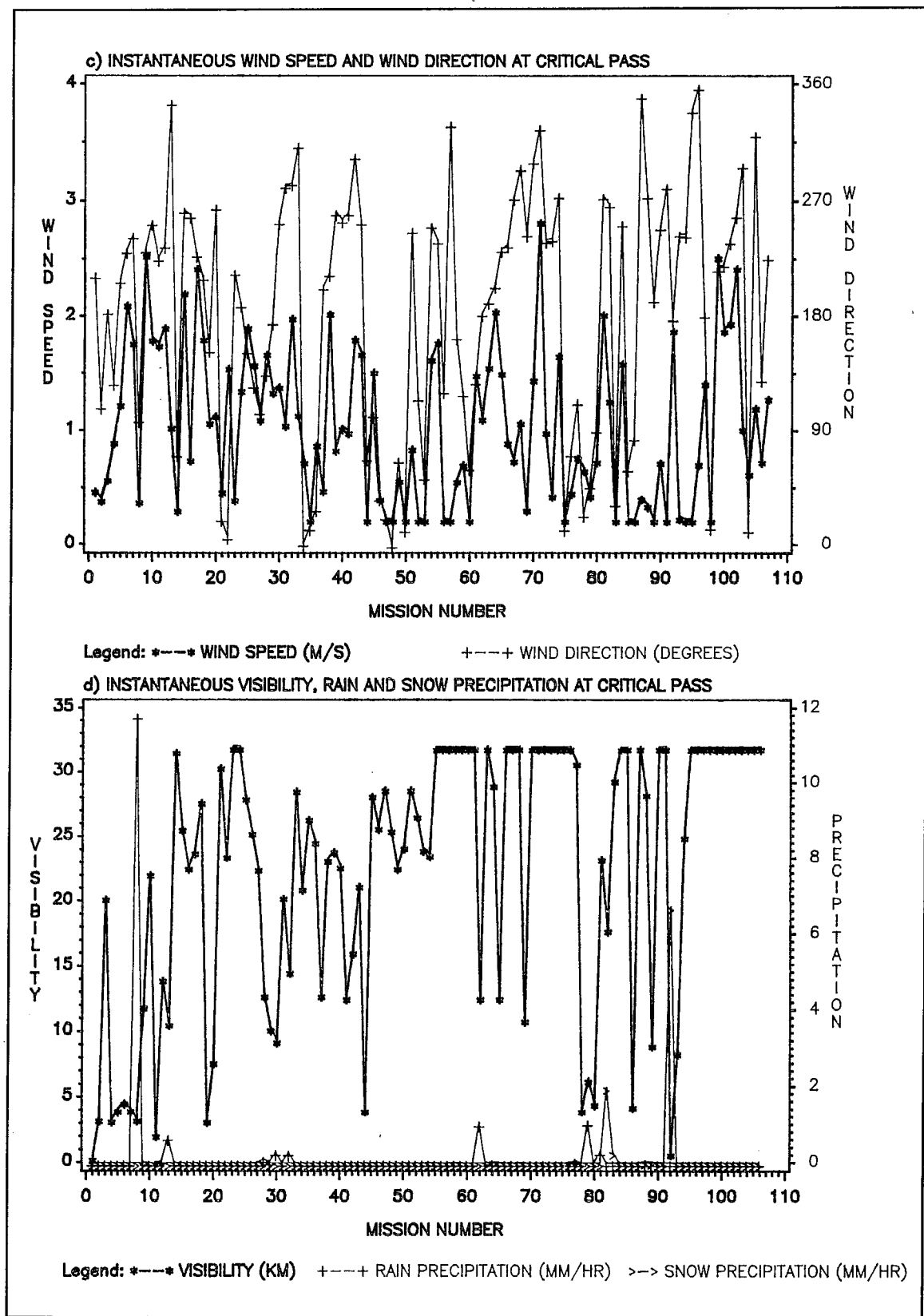


Figure 22. (Concluded)

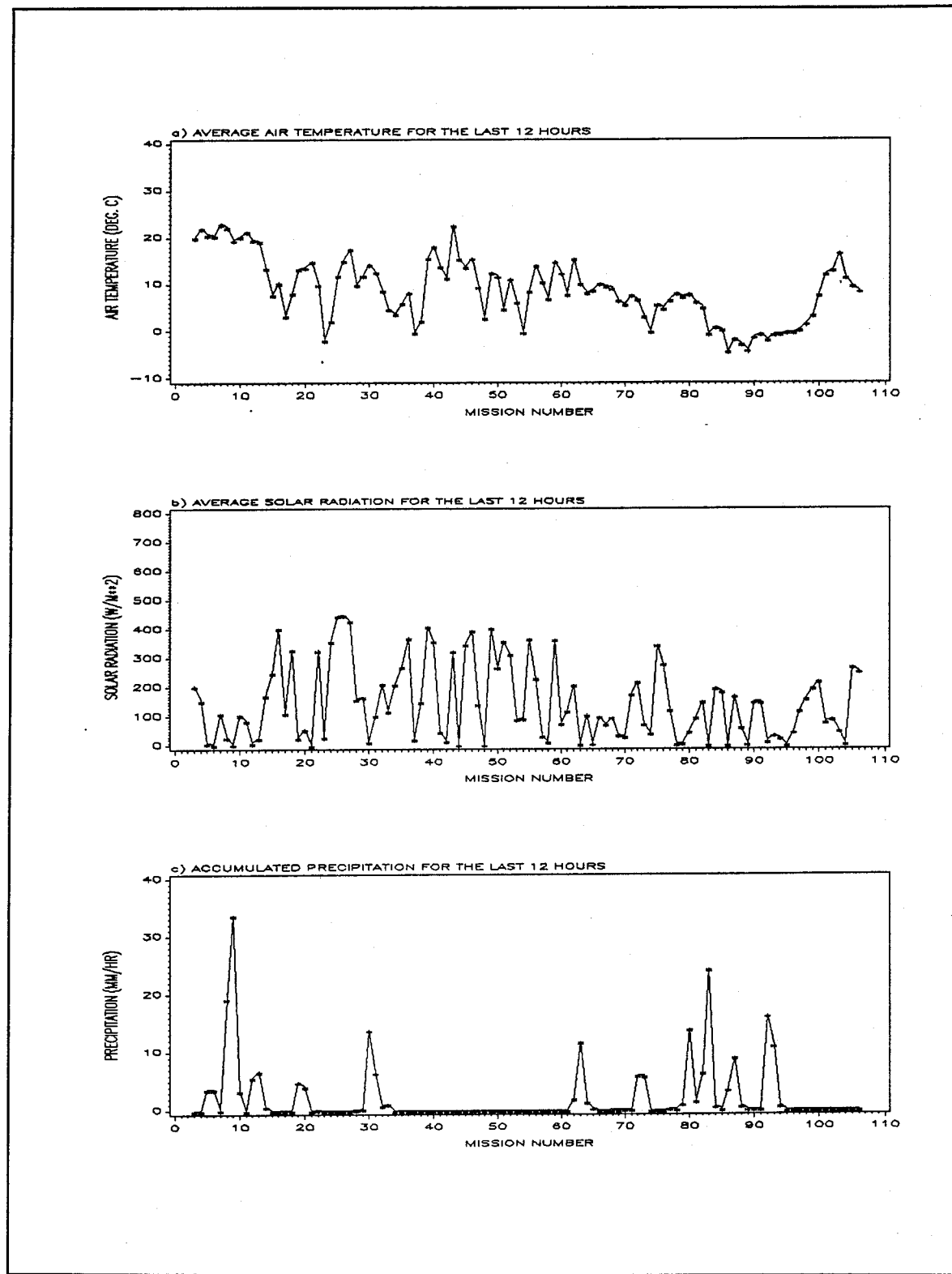


Figure 23. Meteorological conditions prior to critical frame

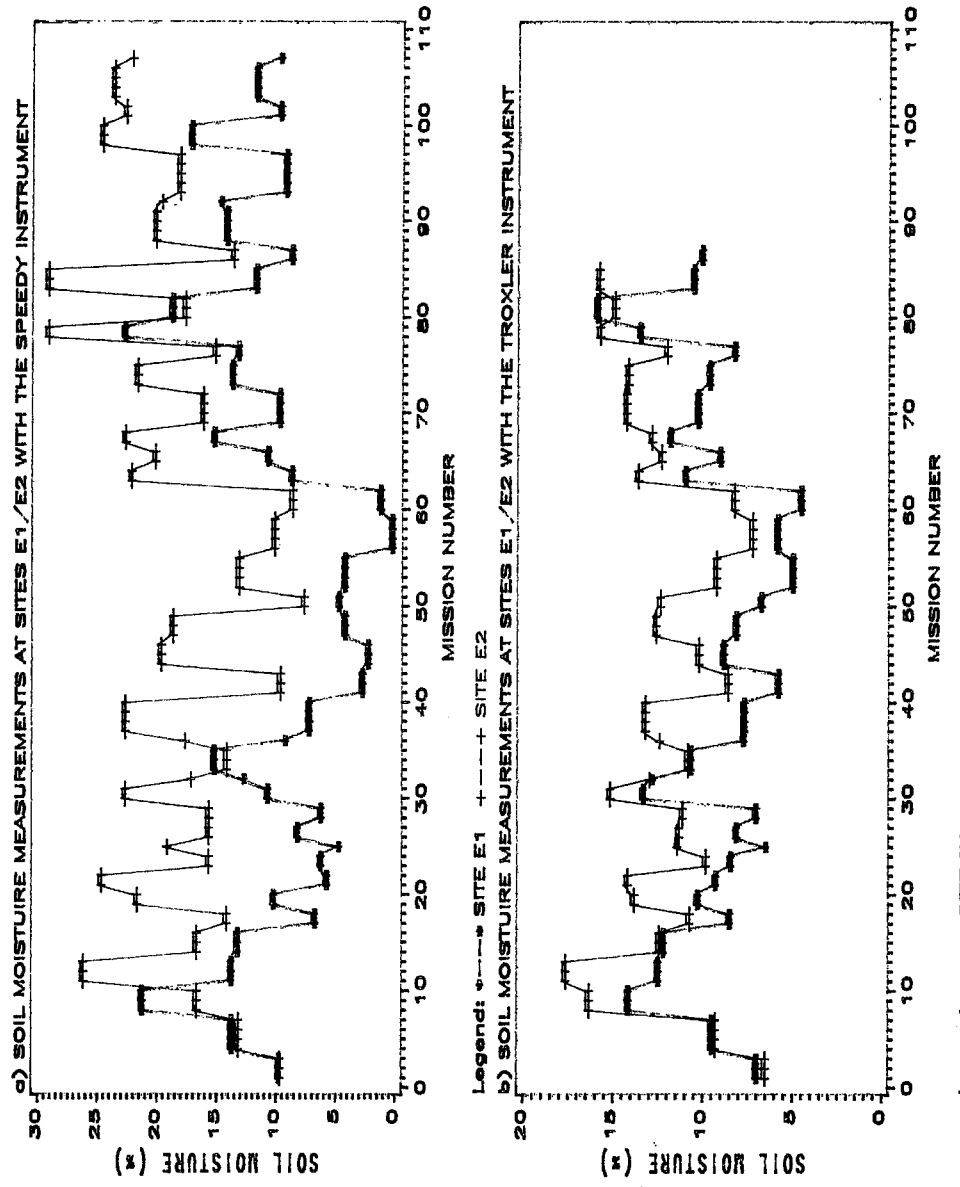


Figure 24. WES soil moisture data for all 107 missions

Table 1
IR Camera Specification

Specification	Wave Band	
	Mid-IR	Far-IR
Model	Thermovision 870 system, infrared camera	Thermovision 782 system, infrared camera
Wavelength band	2 to 5.6 μm	8 to 12 μm
FOV lens	2.48 square deg	3.63 square deg
Screen resolution	140 by 140 square pixels	140 by 140 square pixels
Image resolution	8-bit resolution	8-bit resolution
Radiometric sensitivity	0.1 $^{\circ}\text{C}$ at 30 $^{\circ}\text{C}$ object temperature	0.1 $^{\circ}\text{C}$ at 30 $^{\circ}\text{C}$ object temperature
Radiometric accuracy	$\pm 3\%$ or ± 3 $^{\circ}\text{C}$	$\pm 3\%$ or ± 3 $^{\circ}\text{C}$

Table 2
Imaging Schedule for Grayling 1

Month	Time	Time																																									
		15	16	17	18	19	20	21	22	23	24	25	26	27	28	29	30	1	2	3	4	5	6	7	8	9	10	11	12	13	14	15	16	17	18	19	20	21	22	23	24	25	
0	004	008	011	014														040				052	052	056				076			080												
1	004	008	011	014															050	052	056				067			076															
2	004	008	011	014															050	056		067	069																				
3																		033																									
4																		033																									
5																		047				053			060																		
6	001	005																047				053			060																		
7	001	005																021				041			053																		
8	002	006																021	023			037	042	044	048			058															
9	002	006	009	012														017	023			037	042																				
10	009	012	017	019														017	019			034			054			065															
11	013	013	019															020		038			054			061			070			079											
12		013	020															030		038			061																				
13		015	018	020																																							
14		015	018															024			034																						
15		010																024		028		034		045		051			068	071													
16	003	010	016															022		028			045		051	055			068			077			082								
17	003		016															022	025	026		032		036			055																
18																		025	026	029	031	032	036		049																		
19																		029	031	035		035		046	049		059																
20		007																	035		039		046			059	062																
21		007																		039	043			062			072																
22																				043							064	066		072	075												
23																				040							064	066		075													

Table 3
Summary of Grayling 1 Imagery Data (based on 107 missions)

Wave Bands	Good Images	Good Images after Noise Removed	Bad Or Lost Images	Total
3- to 6- μ m short wave band (SWB)	22%	57%	21%	100%
8- to 14- μ m long wave band (LWB)	37%	46%	17%	100%

Table 4
Different Pair Images Comparison for 10 Images Taken 1 Sec Apart

Pair Image Combination		Lag Time, seconds	T Value, %
Image No.	Image No.		
1	2	1	T ₁
2	3	1	T ₂
1	3	2	T ₃
1	4	3	T ₄
•	•	•	•
•	•	•	•
•	•	•	•
1	10	9	T ₄₅

Table 5
Missions with Visibility Less Than 5 km

Mission Number	Collection Date-Time	Visibility km	Visual Data Availability	Atmospheric Condition
1	15SEP92:07:00:01	0.40	No	Fog
2	15SEP92:09:00:00	3.40	No	Fog
4	16SEP92:01:30:05	3.30	No	Fog
5	16SEP92:07:00:06	4.10	No	Fog
6	16SEP92:09:20:09	4.70	No	Fog
7	16SEP92:20:20:04	4.10	No	Fog
8	17SEP92:02:00:02	3.40	No	Rain
11	18SEP92:01:15:07	2.20	No	Fog
19	21SEP92:12:00:05	3.30	Yes	Fog
44	03OCT92:07:20:07	4.10	No	Fog
78	15OCT92:05:04:10	4.10	No	Fog
80	16OCT92:00:05:04	4.60	No	Fog
86	18OCT92:08:45:09	4.40	Yes	Fog/Snow
92	20OCT92:12:00:02	0.80	Yes	Snow

Table 6**Missions with 12-hr Accumulated Precipitation Greater than 5 mm/hr**

Mission Number	Collection Date-Time	Accumulated Precipitation mm/hr	Average Solar Radiation W/M ²	Average Air Temperature, °C	Troxier,%		Speedy,%	
					E1	E2	E1	E2
8	17SEP92:02:00:02	19	30	22.21	14	17	22	17
9	17SEP92:11:00:02	34	5	19.51	14	17	22	17
12	18SEP92:11:00:02	6	10	19.58	13	18	14	27
13	18SEP92:13:15:09	7	27	19.27	13	18	14	27
30	27SEP92:11:00:08	14	13	14.32	14	15	11	23
31	27SEP92:18:05:07	6	104	12.63	14	15	11	23
63	09OCT92:09:00:09	12	5	10.19	11	14	9	23
72	12OCT92:22:10:08	6	217	6.77	10	15	10	17
73	13OCT92:03:30:04	6	73	3.23	10	14	14	22
80	16OCT92:00:05:04	14	46	7.73	16	15	19	18
82	16OCT92:17:00:06	6	150	5.01	16	15	19	18
83	17OCT92:07:10:10	24	0	-0.61	11	16	12	30
87	18OCT92:21:50:03	9	168	-1.65	10	•	9	14
92	20OCT92:12:00:02	16	13	-1.90	•	•	15	20
93	21OCT92:00:15:05	11	34	-0.68	•	•	10	19

Table 7
Missions with Features Covered with Snow

Mission Number	Collection Date-Time	Grassy Area Covered?	Coniferous Tree Covered?	Deciduous Tree Covered?	Test Track Covered	Visual Data
72	12OCT92:22:10:08	Probably	Probably	Probably	Probably	No
73	13OCT92:03:30:04	Probably	Probably	Probably	Probably	No
82	16OCT92:17:00:06	Yes	No	No	Yes	Yes
83	17OCT92:07:10:10	Probably	Probably	Probably	Probably	No
86	18OCT92:08:45:09	Yes	Yes	Yes	Yes	Yes
87	18OCT92:21:50:03	Probably	Probably	Probably	Probably	No
88	19OCT92:03:25:09	Probably	Probably	Probably	Probably	No
89	19OCT92:09:00:08	Yes	No	No	Yes	Yes
92	20OCT92:12:00:02	Yes	Yes	Yes	Yes	Yes
93	21OCT92:00:15:05	Probably	Probably	Probably	Probably	No
94	21OCT92:02:10:01	Probably	Probably	Probably	Probably	No
95	21OCT92:06:55:01	Probably	Probably	Probably	Probably	No
96	21OCT92:11:15:01	Yes	No	No	No	Yes
97	21OCT92:13:00:07	Yes	No	No	No	Yes
98	22OCT92:01:10:07	Probably	Probably	Probably	Probably	No

Appendix A

Image Data Collection Procedures

The infrared (IR) cameras contain no built-in blackbodies; however, each was recently calibrated by the manufacturer. Further, these DC-restored scanning radiometer cameras require manual setting of the levels and ranges. Consequently, a procedure was employed to verify the accuracy of the radiometric temperature estimates and to ensure that the manually set thresholds of all images were within dynamic range. The field portion of this procedure consisted of the following two steps:

- a. Four active blackbodies were aligned such that they could be directly viewed by the sensors within a single field of view. The blackbody on the extreme left was set to ambient temperature, and the other three blackbodies (left to right) were set to the ambient temperature plus 10, 20, and 30 °C, respectively.
- b. Before and after an imagery data collection mission, the four active blackbodies were imaged by the thermal cameras, and two infrared images were taken: far-IR and mid-IR. Simultaneously, the blackbody temperatures were recorded.

Upon completion of imaging, all scene images were automatically checked to identify those out of dynamic range. Images with more than 2 percent of the brightness values, less than 2 or greater than 253, were rejected.

The accuracy of the factory calibration was examined using these blackbody images by comparing the camera's radiometric temperature estimates with the temperatures measured from the blackbodies. When 90 percent of the absolute errors were under 3 °C, the factory calibration procedures were used for a given excursion. When errors exceeded this level, a corrective procedure was employed. It consisted of a linear adjustment to fit the camera's radiometric temperature estimate to the temperature of the blackbodies. The formula of this correction is as follows:

$$T_{BB} = (a * T_C) + b$$

where:

T_{BB} = physical temperature of blackbody

a = slope estimated by least squares regression

T_C = camera's radiometric estimate of blackbody temperature

b = intercept estimated by least squares regression

When the blackbody temperature estimates could be corrected to meet the above acceptance criteria, the corresponding scene images were used. In the end, only images meeting the accuracy criteria were used for analysis.

These cameras were mounted in a remote-controlled pan and tilt mount atop a 55-ft boom on the WES boom truck.¹ The imaging procedure was first to rotate the boom and the cameras to point at a set of four active blackbodies provided by Eglin Air Force Base and collect image data for each of the two wave bands. Then, the boom was extended to its full height, and thermal cameras were rotated to aim at the Site E area to start the data collection. At the conclusion of the sampling period, the boom and thermal cameras were repositioned to collect a second image of the blackbody. These blackbody images collected at the beginning and end of an imaging period would later be used to check for camera accuracy and make any necessary correction.

¹ To convert feet to meters, multiply number of feet by 0.3048.

Appendix B

Grayling 1 Image Metrics

Appendix C

Instantaneous Meteorological and Terrain Data

MISSION NUMBER	DATE	IMAGE NUMBER	COLLECTED WAVELENGTH (NM)	IMAGE																				
				MEAN	STANDARD	DEVIATION																		
(DEG. C)	(DEG. C)	(DEG. C)	(DEG. C)	(DEG. C)	(DEG. C)	(DEG. C)	(DEG. C)	(DEG. C)	(DEG. C)	(DEG. C)	(DEG. C)	(DEG. C)	(DEG. C)	(DEG. C)	(DEG. C)	(DEG. C)	(DEG. C)	(DEG. C)	(DEG. C)	(DEG. C)	(DEG. C)			
73	13061921:03:30:04	LNB	-6.9	1.1	-1.9	3.2	5.1	0	73	111	100	980	0.4	242	32	0.00	HOME	6	6	14	10	22	14	
74	13061921:10:00:03	LNB	-0.6	1.0	-0.6	4.6	0.0	3.3	267	41	129	983	1.7	275	32	0.00	HOME	6	6	14	10	22	14	
75	13061921:22:40:06	LNB	-2.6	0.4	0.2	5.7	2.7	0	345	180	99	986	0.2	14	32	0.00	HOME	0	0	14	10	22	14	
76	13061921:06:15:01	LNB	0.2	0.4	-0.2	4.8	2.5	0	276	180	100	987	0.5	73	32	0.00	HOME	0	0	14	8	16	12	
77	14061921:17:20:10	LNB	7.1	0.6	9.4	6.6	4.5	0	121	78	90	990	0.8	113	31	0.06	BATH	0	0	14	8	16	12	
78	15061921:05:40:10	LNB	5.3	0.2	6.9	7.9	6.9	0	5	61	100	992	0.7	25	4	0.00	HOME	0	0	23	14	30	16	
79	15061921:11:06:01	LNB	6.3	0.3	7.5	7.2	7.7	0	7	57	100	993	0.4	48	6	1.06	BATH	1	1	16	15	18	15	
80	-	LNB	-	-	6.6	3.6	7.7	7.2	0	46	26	100	988	0.7	91	5	0.00	HOME	14	15	19	16	18	15
81	16061921:14:20:10	LNB	3.6	1.1	3.6	6.1	6.6	210	95	63	100	982	2.0	23	32	0.39	BATH	1	15	19	16	18	15	
82	16061921:17:00:06	LNB	-0.2	0.5	1.4	5.0	5.8	58	150	170	100	983	1.3	248	18	1.94	SNOW	6	20	19	16	18	15	
83	17061921:07:10:10	LNB	-1.2	0.2	-0.7	0.6	1.7	0	0	77	100	994	0.2	33	32	0.28	SNOW	26	31	12	11	30	16	
84	17061921:08:20:01	LNB	0.6	0.6	2.2	0.8	0.2	18	194	99	67	994	1.6	253	32	0.00	HOME	1	25	12	11	30	16	
85	17061921:22:55:03	LNB	-1.3	1.1	4.5	0.3	0.3	-0.2	0	184	97	100	992	0.2	61	32	0.00	HOME	0	5	12	11	30	16
86	18061921:08:45:09	LNB	-7.6	1.3	-3.9	-4.3	-1.6	-0.6	0	0	97	100	992	0.2	85	4	0.00	HOME	4	9	10	14	-	-
87	18061921:21:30:03	LNB	-4.1	0.7	-2.2	-2.2	-2.9	0	168	84	94	995	0.4	351	32	0.00	HOME	9	12	9	10	14	-	
88	19061921:03:25:09	LNB	-6.4	1.2	-3.7	-2.8	-2.5	0	62	84	100	995	0.4	275	28	0.04	SNOW	1	13	15	10	-	-	
89	19061921:09:00:08	LNB	-3.2	0.2	-4.1	-2.8	-2.8	12	4	86	100	997	0.2	194	9	0.03	SNOW	0	9	15	-	-	-	
90	19061921:18:20:01	LNB	0.0	0.5	1.5	1.2	-1.2	-2.3	0	148	76	86	997	0.7	250	32	0.00	HOME	0	0	15	-	-	-
91	19061921:21:55:07	LNB	-3.9	0.6	-1.8	-0.5	-0.5	-2.2	0	148	74	100	995	0.2	282	32	0.00	HOME	0	0	15	-	-	-
92	20061921:22:00:02	LNB	-0.8	0.1	-1.8	-1.9	-1.1	-0.1	40	13	63	989	1.9	179	1	0.71	SNOW	16	18	15	15	-	-	
93	-	LNB	-	-	0.6	-1.3	0	34	21	100	990	0.3	245	9	0.00	HOME	11	20	10	19	-	-		
94	-	LNB	-	-	0.5	-0.7	-1.0	0	22	21	100	991	0.2	245	25	0.00	HOME	1	20	10	19	-	-	
95	-	LNB	-	-	0.8	-0.3	-0.7	0	1	21	100	995	0.2	340	32	0.00	HOME	0	20	10	19	-	-	
96	21061921:11:05:03	LNB	0.0	1.0	2.3	-0.2	-0.5	248	45	41	100	1000	0.37	358	32	0.00	HOME	0	16	10	19	-	-	
97	21061921:13:30:01	LNB	0.3	1.2	3.5	0.3	-0.1	208	117	73	97	1002	1.6	182	32	0.00	HOME	0	4	10	19	-	-	
98	22061921:10:07	LNB	-5.4	1.0	-2.2	1.6	0.9	0	159	125	100	1002	0.2	15	32	0.00	HOME	0	0	18	15	-	-	
99	22061921:16:20:03	LNB	11.2	0.6	12.8	3.4	1.7	116	195	130	70	1003	2.5	218	32	0.00	HOME	0	0	18	15	-	-	
100	22061921:19:00:03	LNB	7.6	1.3	11.5	7.7	2.6	0	218	109	74	1001	1.9	222	32	0.00	HOME	0	0	18	15	-	-	
101	23061921:02:40:01	LNB	7.2	1.4	10.8	12.2	5.9	0	79	109	91	999	2.0	240	32	0.00	HOME	0	0	10	10	23	-	
102	23061921:12:20:03	LNB	17.6	1.3	20.8	13.0	12.1	207	90	121	81	995	2.1	260	32	0.00	HOME	0	0	10	10	23	-	
103	24061921:04:40:05	LNB	4.1	0.6	6.0	6.0	16.7	15.8	48	126	100	969	1.0	296	32	0.00	HOME	0	0	12	12	26	-	
104	24061921:09:00:10	LNB	6.6	0.2	7.9	7.9	11.3	15.2	8	4	128	91	991	0.6	12	32	0.00	HOME	0	0	12	12	26	-
105	24061921:16:20:04	LNB	6.6	0.6	7.9	9.6	11.6	3	266	135	73	993	1.2	322	32	0.00	HOME	0	0	12	12	26	-	
106	24061921:23:31:02	LNB	3.4	0.2	4.9	8.4	8.4	0	251	133	87	993	0.7	131	32	0.00	HOME	0	0	12	12	26	-	
107	25061921:13:55:09	LNB	16.3	0.2	16.1	-	0	169	-	-	100	996	0.5	237	0	0.00	HOME	10	10	23	10	7	10	
108	15SP02:07:06:01	SAB	-	-	-	-	-	-	-	-	-	-	-	-	-	-	-	-	-	-	-	-		

MISSION NUMBER	IMAGE DATE	IMAGE TIME	MEAN AIR TEMPERATURE		MEAN AIR HUMIDITY		MEAN SOLAR RADIATION		MEAN SOLAR RADIATION		MEAN SOIL MOISTURE		MEAN SOIL MOISTURE	
			MEAN	STANDARD DEVIATION	DEVIATION	MEAN	DEVIATION	LAST 12 HRS	LAST 24 HRS	LAST 72 HRS	LAST 72 HRS	LAST 72 HRS	AT E1	AT E2
2	1 SEP 92 17:20:09	S48	24.9	0.6	-	17.3	-	70	-	100	997	0.4	110	3
3	1 SEP 92 10:13:05	S48	20.1	0.3	18.9	22.1	19.4	0	156	168	84	998	0.6	184
4	1 SEP 92 10:13:05	S48	21.1	0.2	19.7	20.7	20.1	0	112	100	996	0.9	126	3
6	1 SEP 92 09:26:09	S48	21.1	0.1	20.1	20.5	20.4	38	5	112	100	994	1.2	209
7	1 SEP 92 20:26:04	S48	19.8	0.3	20.7	21.1	21.0	0	111	56	97	993	2.1	232
8	1 SEP 92 21:22:04	S48	18.5	0.5	22.2	21.1	0	30	56	100	993	1.8	264	4
9	1 SEP 92 11:08:02	S48	19.5	0.1	18.5	20.5	20.3	23	5	52	100	999	0.4	199
10	1 SEP 92 11:08:02	S48	20.2	0.3	20.8	20.8	20.0	3	107	58	94	980	1.8	254
11	1 SEP 92 01:15:07	S48	20.0	0.3	18.8	21.4	19.6	0	66	54	100	986	1.8	226
12	1 SEP 92 11:08:02	S48	17.6	0.2	17.4	19.6	19.7	35	10	58	100	980	1.9	236
13	1 SEP 92 01:15:07	S48	-	-	15.2	19.3	19.6	58	27	56	100	980	1.0	346
14	1 SEP 92 01:15:07	S48	9.1	0.7	16.8	15.0	0	173	98	92	997	0.3	73	32
15	1 SEP 92 11:08:07	S48	16.9	1.7	14.2	7.0	10.0	627	250	984	996	2.2	263	26
16	1 SEP 92 18:20:03	S48	13.1	0.6	12.6	9.5	7.1	403	213	63	993	0.8	253	26
17	2 SEP 92 11:08:06	S48	17.1	2.1	13.8	3.3	7.0	590	112	229	69	992	2.4	269
18	2 SEP 92 11:30:09	S48	23.7	2.7	19.0	6.2	7.6	481	329	262	990	1.8	211	28
19	2 SEP 92 11:08:08	S48	-	-	14.2	13.3	14.6	102	26	163	39	983	1.1	154
20	2 SEP 92 11:08:08	S48	16.3	0.4	15.9	13.6	14.6	14.6	56	125	100	983	1.1	266
21	2 SEP 92 10:15:09	S48	9.6	0.5	8.9	15.0	14.7	0	2	49	92	984	1.1	21
22	2 SEP 92 11:08:08	S48	10.2	1.3	12.6	14.5	12.6	14.5	328	170	70	993	1.6	9
23	2 SEP 92 10:15:08	S48	7.8	1.9	14.4	10.0	14.4	7.8	258	28	183	97	0.4	215
24	2 SEP 92 11:08:04	S48	20.9	4.4	13.7	2.4	3.2	598	359	254	47	1002	1.4	190
25	-	S48	-	-	17.9	11.9	8.5	175	447	237	44	1003	1.9	153
26	-	S48	-	-	19.5	15.2	12.3	179	450	237	46	998	1.6	126
27	2 SEP 92 22:20:07	S48	11.3	0.7	11.4	17.7	12.2	0	430	227	92	997	1.1	105
28	2 SEP 92 14:26:20	S48	15.9	0.2	15.7	9.9	11.3	121	159	134	87	991	1.7	135
29	2 SEP 92 11:08:02	S48	14.4	0.2	13.7	11.9	10.8	0	167	96	99	989	1.4	176
30	-	S48	-	-	11.7	14.3	14.4	72	13	70	100	986	1.4	255
31	2 SEP 92 18:05:07	S48	13.1	0.1	12.4	12.6	13.3	28	104	54	85	992	1.1	283
32	2 SEP 92 18:05:04	S48	12.0	0.9	6.2	8.7	7.3	0	212	111	93	995	2.0	285
33	-	S48	-	-	3.3	4.8	6.2	0	118	107	95	998	1.2	315
34	2 SEP 92 15:20:01	S48	15.7	1.9	9.5	3.7	3.9	215	210	119	66	1001	0.7	1
35	-	S48	-	-	5.8	6.0	4.2	0	269	135	42	999	0.2	27
36	3 SEP 92 18:05:10	S48	20.8	1.4	15.0	8.3	5.8	127	370	189	55	999	0.9	25
37	3 OCT 92 00:10:03	S48	8.7	1.4	6.5	-0.2	5.0	207	21	100	997	0.5	204	13

IMAGE	MEAN AIR			MEAN SOLAR			MEAN SOIL			MEAN TRODOL SOIL		
	IMAGE	MEAN	STANDARD	AIR TEMPERATURE	LAST 24HRS	SOLAR RADIATION	LAST 24HRS	SOIL MOISTURE	LAST 24HRS	SOIL MOISTURE	LAST 24HRS	SOIL MOISTURE
SESSION	DATE	IMAGE	COLECTED	UNIVERSITY	TEMPERATURE (C)	DEVIATION (C)	TEMPERATURE (C)	LAST 24HRS	RADIATION (W/m ²)	LAST 24HRS	RADIATION (W/m ²)	RADIATION (W/m ²)
38	01/01/92-12:00:00	SAB	23.5	2.3	16.9	1.3	16.0	15.7	8.0	0	409	212
40	01/01/92-22:15:00	SAB	15.4	1.3	16.8	0.6	16.2	9.0	0	357	205	80
41	01/01/92-22:30:07	SAB	-	-	9.5	-0.2	11.8	11.5	0	48	205	76
42	01/01/92-22:45:00	SAB	-	-	15.4	1.4	11.4	13.6	21%	15	210	100
43	01/01/92-22:55:08	SAB	19.1	0.8	17.3	2.2	16.5	17.3	0	323	169	85
44	01/01/92-00:00:07	SAB	11.6	0.5	6.4	1.4	7.4	7.4	0	2	169	100
46	01/01/92-10:00:00	SAB	27.8	3.4	20.2	13.7	18.4	18.4	4.2	347	217	55
47	01/01/92-00:20:12	SAB	6.9	0.6	1.2	1.2	11.5	15.3	0	395	194	57
48	01/01/92-10:30:04	SAB	4.9	0.7	9.4	10.6	10.6	10.6	0	141	197	100
49	01/01/92-11:00:03	SAB	14.2	1.2	11.1	12.5	7.7	7.7	0	2	197	100
50	01/01/92-11:15:03	SAB	-	-	-1.5	11.7	7.1	7.1	0	403	203	65
51	01/01/92-11:30:03	SAB	-	-	16.6	4.4	5.0	5.0	380	265	202	100
52	01/01/92-00:45:04	SAB	7.0	1.1	2.2	11.1	6.0	6.0	0	312	225	52
53	01/01/92-11:50:00	SAB	-	-	-2.5	6.2	4.9	4.9	0	100	100	0
54	01/01/92-11:00:01	SAB	19.1	2.3	12.1	-0.2	5.3	4.48	0	202	100	99
55	01/01/92-11:20:01	SAB	25.6	1.4	19.5	8.6	6.8	6.8	0	224	77	100
56	01/01/92-00:55:02	SAB	12.0	0.9	7.3	14.0	7.2	7.2	0	366	206	53
57	01/01/92-01:55:00	SAB	10.0	0.9	7.8	10.0	8.6	8.6	0	230	187	100
58	01/01/92-10:00:05	SAB	8.0	0.5	8.0	6.9	10.2	8.5	0	32	187	96
59	01/01/92-12:00:00	SAB	15.1	1.3	12.6	8.7	8.1	8.1	0	12	193	96
60	01/01/92-12:15:00	SAB	9.2	1.3	4.0	12.4	11.0	11.0	0	364	182	65
61	01/01/92-00:25:01	SAB	-	-	11.3	0	7.5	7.5	0	100	99	0
62	01/01/92-00:40:09	SAB	15.5	0.6	9.1	9.1	9.6	9.1	0	991	62	32
63	01/01/92-00:50:03	SAB	16.4	0.2	13.2	11.4	11.4	11.4	0	207	103	100
64	01/01/92-11:00:07	SAB	-	-	12.7	10.2	12.7	14	5	105	99	99
65	01/01/92-11:10:00	SAB	-	-	7.4	8.1	8.6	8.6	0	105	55	100
66	01/01/92-11:20:00	SAB	-	-	9.3	8.7	8.1	8.1	0	100	55	100
67	01/01/92-00:25:01	SAB	12.6	0.2	7.5	8.1	9.1	9.1	0	97	100	0
68	01/01/92-00:40:09	SAB	12.9	0.2	6.2	9.6	9.1	9.1	0	75	102	49
69	01/01/92-11:25:01	SAB	15.5	0.6	9.1	9.1	9.6	9.1	0	100	99	0
70	01/01/92-11:30:03	SAB	8.6	0.9	4.2	6.5	7.3	7.3	0	355	49	100
71	01/01/92-11:30:07	SAB	12.1	0.2	10.0	5.6	6.9	6.9	0	257	30	60
72	01/01/92-12:00:04	SAB	14.1	0.6	8.2	7.6	7.0	7.0	0	197	105	62
73	01/01/92-00:25:01	SAB	-	-	1.6	6.8	5.7	5.7	0	217	111	100
74	01/01/92-00:40:09	SAB	-	-	-1.9	3.2	5.1	5.1	0	73	111	100

MISSION NUMBER	DATE IMAGE COLLECTED	IMAGE NUMBER (FIG. C)	IMAGE STANDARD DEVIATION (FIG. C)	MEAN AIR TEMPERATURE			MEAN SOLAR RADIATION			BAROMETRIC PRESSURE			MEAN PRECIPITATION			MEAN VISIBILITY			MEAN SPEEDY SOIL MOISTURE			
				LAST 12HRS	LAST 24HRS	LAST 48HRS	(deg. C)	(deg. C)	(deg. C)	(W/m ²)	(W/m ²)	(W/m ²)	(mm/hr)	(mm/hr)	(mm/hr)	(km)	(km)	(km)	(percent)	(percent)	(percent)	
74	130C192:19:00:03	546	9.4	0.9	4.6	-0.0	3.3	2.67	4.1	129	70	943	1.7	275	32	0.00	0	6	14	10	22	14
75	130C192:22:00:01	546	5.4	0.5	0.2	5.7	2.7	0	345	180	99	966	0.2	14	32	0.00	0	0	14	10	22	14
76	-	546	-	1.0	4.8	2.5	0	270	180	100	967	0.5	73	32	0.00	0	0	8	16	12	12	
77	140C192:17:00:10	546	12.6	0.3	9.4	6.6	4.5	0	121	78	90	990	0.8	113	31	0.06	0	0	14	8	16	12
78	-	546	-	6.9	7.9	6.9	0	5	61	100	992	0.7	25	4	0.00	0	0	23	14	30	16	
79	150C192:11:00:01	546	12.0	0.2	7.5	7.2	7.7	0	7	57	100	993	0.4	48	6	1.06	0	1	23	14	30	16
80	-	546	-	6.8	7.7	7.2	0	46	26	100	985	0.7	91	5	0.00	0	0	15	19	16	15	
81	-	546	-	6.1	6.4	6.4	0	210	95	63	100	982	2.0	274	23	0.29	0	15	19	16	15	
82	160C192:17:00:06	546	6.6	0.4	5.0	5.8	58	150	77	100	983	1.3	268	18	1.96	RAIN	1	6	20	19	16	15
83	170C192:07:10:10	546	4.4	0.3	-0.6	1.7	0	0	77	100	994	0.2	33	30	0.28	SNOW	26	31	12	11	30	16
84	170C192:18:20:01	546	6.6	1.4	2.2	0.8	0.2	16	194	99	97	994	1.6	253	32	0.00	0	0	12	11	30	16
85	170C192:22:15:03	546	1.9	0.8	-4.5	0.3	-0.2	0	164	97	100	992	0.2	61	32	0.00	0	5	12	11	30	16
86	180C192:08:15:09	546	4.5	1.6	-3.9	-1.6	0	0	97	100	992	0.2	85	4	0.00	0	4	9	10	14	-	
87	190C192:13:00:03	546	3.1	0.5	-2.2	-1.7	0	163	64	94	995	0.4	351	32	0.00	0	9	12	11	30	16	
88	190C192:13:25:09	546	0.7	0.9	-3.7	-2.8	0	235	0	62	84	100	995	0.4	275	28	0.04	0	13	15	-	
89	190C192:19:00:08	546	5.1	-2.3	-4.1	-2.8	12	4	86	100	997	0.2	194	9	0.03	SNOW	0	2	15	-		
90	190C192:18:20:01	546	4.9	0.4	1.5	-2.3	0	143	76	86	997	0.7	250	32	0.00	0	0	15	-			
91	-	546	-	-1.6	-0.5	-2.2	0	143	76	100	995	0.2	282	32	0.00	0	0	15	-			
92	200C192:12:00:02	546	5.9	0.1	-0.1	-1.9	40	13	63	100	989	1.7	179	1	4.71	SNOW	16	15	-			
93	-	546	-	0.6	-0.7	-1.3	0	36	21	100	990	0.3	265	9	0.00	0	11	20	19	-		
94	-	546	-	0.5	-0.6	-1.0	0	22	21	100	981	0.2	265	25	0.00	0	1	20	19	-		
95	210C192:06:35:01	546	5.0	0.3	-0.3	-0.3	0	21	50	99	995	0.2	340	32	0.00	0	0	20	19	19		
96	-	546	-	2.3	-0.2	-0.5	248	45	41	100	1000	0.7	358	32	0.00	0	16	10	-			
97	210C192:13:00:07	546	7.6	0.9	3.5	0.3	-0.1	208	117	73	97	1002	1.4	182	32	0.00	0	4	10	-		
98	220C192:10:00:10	546	4.0	0.7	-2.2	1.6	0.9	0	159	125	100	1002	0.2	15	32	0.00	0	0	18	-		
99	220C192:16:20:03	546	20.2	0.7	12.8	3.4	1.7	114	195	130	70	1003	2.5	218	32	0.00	0	0	18	-		
100	220C192:19:00:01	546	13.4	0.9	11.5	7.7	2.6	0	218	109	74	1001	1.9	222	32	0.00	0	0	18	-		
101	230C192:02:40:01	546	15.0	0.6	10.6	12.2	5.9	0	70	109	91	999	2.0	240	32	0.00	0	10	19	-		
102	230C192:12:20:03	546	24.8	1.2	20.6	13.0	12.1	207	90	121	81	995	2.4	260	32	0.00	0	10	20	-		
103	240C192:16:40:05	546	12.5	0.6	8.0	16.7	15.8	0	48	126	100	989	1.0	208	32	0.00	0	12	24	-		
104	240C192:09:00:10	546	12.0	0.1	7.9	11.3	15.2	6	4	128	91	991	0.6	12	32	0.00	0	0	12	-		
105	240C192:18:20:04	546	11.9	1.4	7.9	9.6	11.6	3	268	135	73	993	1.2	322	32	0.00	0	12	24	-		
106	240C192:23:40:02	546	5.2	0.2	4.9	8.4	6.8	0	251	133	87	993	0.7	131	32	0.00	0	12	24	-		
107	-	546	-	11.1	-	-	-	169	-	-	63	990	1.3	227	-	-	-	10	-	25	-	